OULUN YLIOPISTO
UNIVERSITY of OULU

DEGREE PROGRAMME IN WIRELESS COMMUNICATIONS ENGINEERING

MASTER'S THESIS

RF SYSTEM MODEL FOR IN-BAND FULL DUPLEX COMMUNICATIONS

Author   Parisa Nouri

Supervisor   Professor Aarno Pärssinen

Second Supervisor   Risto Vuohtoniemi

August, 2016

ABSTRACT

In recent years by increasing the demands for communication services various technologies are examined in order to improve the throughput and spectrum efficiency of the wireless communication systems. For improving the performance a communication network, system deficiencies such as transmitter and receiver impairments need to be removed or compensated. One way to improve the network efficiency is to employ full duplex technology. Full duplex technology doubles the network capacity compared to the case when typical frequency division duplexing (FDD) or time division duplexing (TDD) are employed in a transceiver design. Although full duplex (FD) technology has enhanced the performance of the radio communication devices, the main challenge in full duplex communication is the leaking self-interference signal from the transmitter to the receiver. Different methods are employed to suppress the self-interference signal in digital and analog domains which are categorized as passive or active cancellations. These techniques are discussed in this thesis in order to understand from which point in the propagation path, the required signal for cancellation can be taken and how those techniques are employed in digital and analog domains. For having a good self-interference cancellation (SIC) both analog and digital cancellation techniques are needed since typical digital suppression method is low complex and somewhat limited. In this thesis, first we start with discussing about the full duplex technology and the reason why it has become popular in recent years and later full duplex deficiencies are examined. In the following chapters different cancellation methods are introduced and some results are provided in Chapter 5.

Keywords: full duplex, self-interference, electrical balance duplexer, active and passive cancellation.

TABLE OF CONTENTS

FOREWORD

This thesis work was carried out at the Centre for Wireless Communications of University of Oulu, Finland. The aim of this thesis work is to design an RF system model for in-band full duplex communications and compare two different RF self-interference cancellation techniques. The target is to find out how much isolation can be provided with each model and how to improve the isolation between the transmitter and receiver chains.

Here, I would like to gratefully acknowledge both of my supervisors Professor Aarno Pärssinen and Lic.Tech. Risto Vuohtoniemi for offering invaluable advices and their support throughout this thesis. Special thanks to Lic.Tech. Visa Tapio and Timo Kumpuniemi for the guidance and invaluable discussions during this thesis work. Finally, I also need to thank my parents for all the moral support during my studies.

LIST OF ABBREVIATIONS AND SYMBOLS

ADC	Analog-to-digital converter
ADS	Advanced design system
BAW	Bulk acoustic wave
BB	Base band
BER	Bit error rate
BW	Bandwidth
CMOS	Complementary metal oxide semiconductor
CSMA	Carrier sense multiple access
EB	Electrical balance
EBD	Electrical balance duplexer
EM	Electromagnetic
EMI	Electromagnetic interference
EVM	Error vector magnitude
FD	Full duplex
FDD	Frequency division duplexing
FS	Full scale
HPA	High power amplifier
IBFD	In-band full duplex
ICP	Input compression point
IF	Intermediate frequency
IIP	Input intercept point
IIP2	2nd order input intercept point
IIP3	3rd order input intercept point
IL	Insertion loss
IM3	Third-order intermodulation
LNA	Low noise amplifier
LO	Local oscillator
LPF	Low pass filter
LS	Least square
MAC	Medium access control
NF	Noise figure
PA	Power amplifier
PAPR	Peak-to-average power ratio
PLF	Polarization loss factor
RF	Radio frequency
RSI	Residual self-interference
SAW	Surface acoustic wave
SI	Self-interference
SIC	Self-interference cancellation
SSINR	Signal-to-self-interference-plus-noise-ratio
TDD	Time division duplexing
VCO	Voltage controlled oscillator
VGA	Variable gain amplifier
VM	Vector modulator

b	Number of bits at ADC
$c(t)$	Transmit coupled signal
d	Delay
H_{SI}	Self-interference channel
$\hat{H}_{SI}$	Least square estimate of self-interference channel
h_i	TX-to-RX channel
h_{SI}	Channel between SIC chain and adder block
$H_{SI,n}$	Self-interference channel related to nth baseband signal
L_{ret}	Return loss
n	Odd harmonics of baseband signal
P_{RX}	Power of receiver
P_{TX}	Power of transmitter
P_{ANT}	Power of antenna
P_{BAL}	Power of balance network
P_{in}	Input power
P_{out}	Output power
P_{quant}	Quantization noise power
P_{target}	Total power of the signal at the input of analog-to-digital converter
r	Received signal
$\hat{r}$	Down converted signal at the receiver
SNR_{ADC}	Signal-to-quantization-noise ratio
S_{12}	Reverse transmission coefficient
S_{21}	Forward transmission coefficient
V_{RX}	Receiver voltage
V_{TX}	Transmitter voltage
V_x	Center tap swing voltage
$\tilde{x}$	Analog baseband signal
$\hat{x}$	Amplified up converted analog signal
Z_{RX}	Receiver impedance
Z_{ANT}	Antenna impedance
Z_{TX}	Transmitter impedance
Z_{BAL}	Balance network impedance
z	Noise
$Z_{ind,p}$	Self-inductance impedance
Z_L	Impedance of load signal
Z_O	Impedance of reference signal
α	Attenuation
γ	Power ratio
Γ	Reflection coefficient
ε	Attenuation
$\hat{\rho}_w$	Polarization unit vector of the incoming wave
$\hat{\rho}_a$	Polarization unit vector of the antenna
Ψ_p	Angle between $\hat{\rho}_w$ and $\hat{\rho}_a$
$\phi_{TX}(t)$	Phase noise process of oscillator at transmitter
$\phi_{RX}(t)$	Phase noise process of oscillator at receiver

1. INTRODUCTION

Two different techniques are used in 3G/4G radios to provide a good isolation between transmitter and receiver ports. Transmitter and receiver can perform concurrently through the frequency division duplexing (FDD) technique which allocates different frequencies to transmitter (TX) and receiver (RX) ports or they can work with the same carrier frequency but in different time slots which refers to time division duplexing (TDD) [1]. In TDD technique, a great amount of bandwidth can be utilized for downloading and also uploading which is beneficial for mobile internet usage. Through the FDD better reception and less interference are achievable.

A bi-directional communication over a solitary route is possible through the duplexer. A duplexer is a 3-port filtering device which provides a good isolation between TX/RX ports while they are sharing a single antenna and so the receiver does not go to the saturation state [2]. Two bandpass filters in parallel are considered in duplexer structure. One filter enables the transmission from the transmitter to the antenna and the second filter provides the communication between the antenna and the receiver; so, the TX and RX donot communicate straightly [3]. All in all, we could say that the transmitter and receiver are coupled to the antenna while the isolation is kept between the TX and RX sides.

Diplexer detaches two distinct frequencies at the receiver side while combines them at the transmitter side. Diplexer can perform properly if these frequency bands are sufficiently far from each other in the the frequency domain of operation. Since both duplexer and diplexer are a 3-port device consist of two filters, sometimes duplexers are called diplexer although there are some differences between them [4].

Today's wireless networks have to combat with an interference signal caused by the transmitter to the receiver side in a radio transceiver. Therefore, we can use duplexers based on surface acoustic wave (SAW) or bulk acoustic wave (BAW) filters to achieve a good isolation between the transmitter and receiver ports.

While SAW filter is a passive device which synthesizes a low insertion loss (IL) with a good rejection, it is bulky and frequency regulation is impossible; hence, numerous duplexers are needed for different supported bands and they are also considered as an obstacle for duplexer integration in complementary metal oxide semiconductor (CMOS) process [2]. Based on these mentioned specifications of SAW filters, electrical balance (EB) has become an alternative to these filters in order to find a better integrity in duplexers and be able to tune the frequency in addition to a high TX-to-RX isolation and insertion loss [5].

There are two choices when we want to set up our network equipment. In half duplex, the transceiver has the ability to send and receive at different frequency and time slots while in full duplex, data is sent and received concurrently on a common frequency. In order to decide which method is desirable for our network infrastructure, we need to evaluate various factors such as speed, homogeneous environments, stability and the needs of the end users. Nowadays because of the growth in network, the demand for wireless communications simultaneously on a same frequency between transmitter and receiver is increased. As discussed earlier, simultaneous packet transmission is possible through full duplex which doubles the network capacity as resources in both frequency and time domains are effectively used [6], [7]. Full duplex brings multiple benefits which are discussed in details in [6]. Different networks such

as carrier sense multiple access (CSMA) and multi-hop networks can improve their performance through full duplex. In CSMA protocols, network devices listen to the channel before transmitting. Therefore, if the channel is sensed to be engaged, the transmission is postponed to avoid collisions. If two devices try to communicate simultaneously, collision occurs and so they need to wait for a random time slot then they start transmitting again. In multi-hop networks, communication between source point and destination point is carried out through two or more wireless hops and they need to relay data from one route to another. Based on FD approach, they can resolve the problem of collision in order to transmit and receive concurrently and achieve a better throughput.

Major problem in FD is related to self-interference (SI) as we utilize a common antenna shared between transmitter and receiver or two antennas located close to each other [8]. Self-interference cancellation can be done in two domains, passive and active suppression [9]. In order to attain a high SIC, both domains can be used together in FD operation [9]. Passive suppression technique has a significant role in SIC since majority of the overall cancellation is done in this domain [10]. In passive cancellation approach the interference signal level is mitigated prior to be processed at the receiver [9], [11], [12] while active cancellation is carried out after receiving the transmitted signal. A copy of baseband signal is attenuated and phase shifted via a second transmission wire and then added to the received signal [13], [9]. Digital and analog cancellations are considered as an active cancellation techniques [9]. Digital cancellation technique does not have the capability of canceling a strong self-interference signal since its power leads to the saturation of analog-to-digital converters (ADC).

The first type of full duplex transceiver is designed with two transmit antennas and one receiver antenna which suppresses the unwanted signal through RF and antenna cancellation techniques [14]. FD operation consists of different parts such as antenna, radio frequency (RF) and digital cancellation [15], [16], [17]. In addition to all merits of FD in wireless networks, this approach still has its own challenges as well. Cancellation is done in several stages in analog and digital domains and as a result, the implementation price increases [15], [16], [17]. Antenna in FD behaves as frequency selective so FD has a limited range of operation and suppressing the interference out of the range of self-interference cancellation (SIC) in the recipient is impossible.

Several techniques are studied to find a good TX-to-RX isolation. In this thesis work, we focus on two self-interference cancellation techniques that authors in [18] have also studied earlier. In radio frequency (RF) with an electrical balance circuit, a hybrid transformer is used in order to suppress the unwanted signal in radio apparatuses [18]. Therefore, the power which comes from the power amplifier (PA) is divided equally between antenna and balance circuit which reduces the amount of transmitted power and 3 dB loss in additions to the hybrid transformer loss is generated [18]. In a balance circuit, an analog tunable resistor and a digital adjustable capacitor are considered in parallel in order to control the impedance of the balance network to follow the antenna impedance alterations to restrict the amount of SI signal leaks from the TX to RX [18].

In the real world of telecommunications, the antenna impedance varies as the environment conditions are not stable during the communications. For this reason, in addition to the above-mentioned approach, authors in [1] have examined an algorithm to automatically tune the balance network and antenna impedances for a desired level of RF SIC.

In the second approach, RF SIC is possible via a dual-polarized dual-feed antenna [18]. Antennas can have different polarization types which affects the transferred energy from PA to the low noise amplifier (LNA). If two electromagnetic waves have the same polarization, the maximum energy is transmitted from the TX to the RX port while with different polarizations, TX power is suppressed and less energy arrives at the receiver. The best case of having no power transmission is the orthogonal polarization [18], [19]. There are two approaches to attain orthogonal polarizations. We can use two separated antennas [18], [10] or a dual polarized antenna [18].

The aim of this thesis is to study different radio frequency (RF) implementation options for a practical TX-to-RX isolation in case of full duplex and evaluate its impact to RF system and radio system design. The idea of this work is to provide proper and realistic models of different TX canceling options for full duplex test bench. In this thesis, different cancellation techniques are compared and a RF model for full duplex communications is provided.

2. FULL DUPLEX TECHNOLOGY

In 1998, the first presentation of full duplex employed for the narrowband communication networks was exhibited [20]. Other authors in [21], [22], [23], [24] and [25] improved this technique for wider channel bandwidths or for the case of having several transmit antennas. Full duplex technology has several advantages such as increasing the link capacity, transmission security, spectrum usage and decreasing the delay time in multi-hop networks [6].

In the following sections, first we talk about the self-interference signal and then the transceiver architecture. In the third section transceiver impairments in the presence of full duplex are examined. Finally, different methods for self-interference cancellation are studied.

2.1. Self-interference Signal

In this section we present several reasons of generating self-interference signal. If a mismatch happens as a result of a bad connection between the duplexer and antenna through the transmision line, a direct path between TX and RX ports will appear and some amount of power leaks from transmitter to the receiver which cause some problems such as saturation and distortion at the receiver [26].

The second reason of generating SI signal is due to the mismatch between antenna's input and transmission line impedances. Therefore, some power is reflected from TX to the RX through the second unwanted path. In case of having a strong reflected signal, distortion and saturation will happen at the receiver side [26]. The amount of reflection is measured by the reflection coefficient Γ. The reflection coefficient Γ is equal to $(Z_L - Z_O)/(Z_L + Z_O)$ where Z_L and Z_O are the load impedance and the reference impedance respectively. Another parameter which indicates how good a full duplex system works is the return loss L_{ret} which is equal to $-20 \log |\Gamma|$. If the antenna matches properly to the transmission line, FD system works satisfactory due to the high level of L_{ret} [27].

Finally, reflections from the environment cause the self-interference signal and they create less amount of self-interference signal in comparison with two other mentioned reasons [26]. However, we need to cancel even small amount of reflections since they restrict the RF cancellation capability in practical cases.

All these three mentioned reasons are shown in Figure 1 [26]. Although working with a joint RF carrier brings some problems such as SI signal, it still has its own merits in FD communications. In this architecture, duplexing filter is substituted with a circulator and greater output is attained [28] also network layers and efficiency of a medium access control (MAC) wireless networks is developed [29].
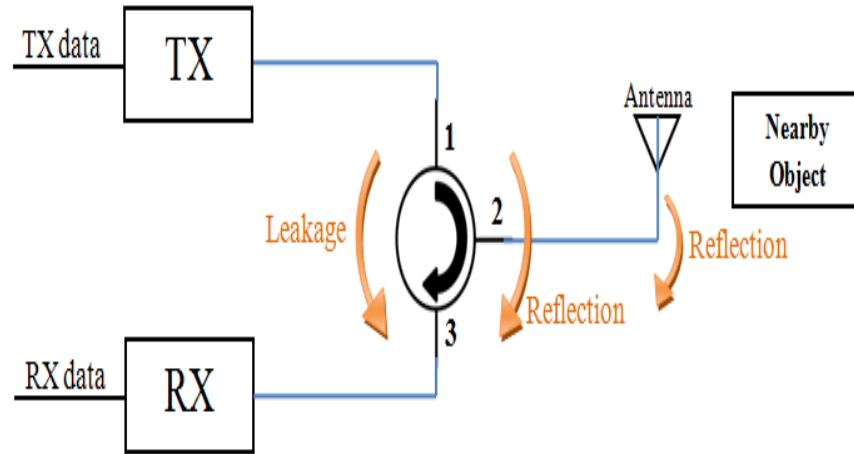
Figure 1. Full duplex transceiver with a circulator. Also three factors of generating self-interference signal are indicated.

2.2. Transceiver Architecture

In radio communications, radio refers to an electronic device that transmits or receives an electromagnetic signal. A radio transceiver comprises both a transmitter and a receiver. In typical transmitters three essential functions such as power amplification, modulation and also frequency conversion take place. There are different transmitter architectures which of each is employed for specific purposes based on the power efficiency, spectral efficiency and modulation accuracy requirements. In all of these transmitter architectures since no complicated filters are required, attaining full integration is feasible. Different configuration of transmitter is listed in Table 1 [30].

Table 1. Specifications of different transmitter configurations

Architecture	Complexity	Power Consumption
Direct conversion	Low	Major power is drawn by PA
Offset direct conversion	Moderate	Major power is drawn by PA
Direct modulation	Very low	Major power is drawn by PA
Impulse radio	Very low	Very low

There are several criterias for choosing the suitable transmitter architecture such as relationship between the output power and system efficiency, linear behavior of the model, appropriate number of oscillators and filters, integrity, etc [31]. Different transmitter architectures are discussed in this section.

- Direct conversion
  Direct conversion transmitter architecture is shown in Figure 2 [31] which has a simple configuration since a few components are needed and provides a high integrity. In this structure, baseband signals are converted straightly to the RF-frequency. But strong signal at the output of power amplifier has a noticeable perturbative effect on the local oscillator in a way that the local oscillator fre-

quency is dragged away from the desired value [30]. Local oscillator (LO) frequency is the same as the output carrier frequency [31].
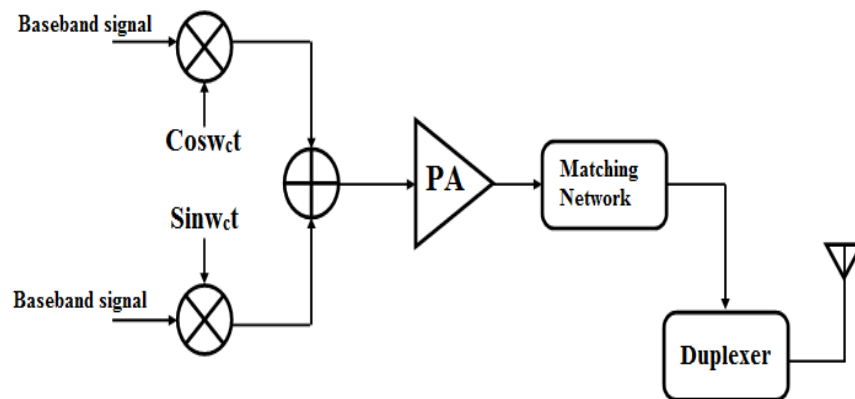

Figure 2. Direct conversion transmitter configuration.

- Offset direct conversion
  This architecture improves the efficiency of direct conversion transmitter via detracting the effect of PA output on the LO by employing an offset local oscillator direct conversion structure. In this architecture which is shown in Figure 3 [30], LO involves two lower frequency signals. In Figure 3 [30] two bandpass Filter (BPF), a voltage controlled oscillator (VCO) are employed and IF means the intermediate frequency.
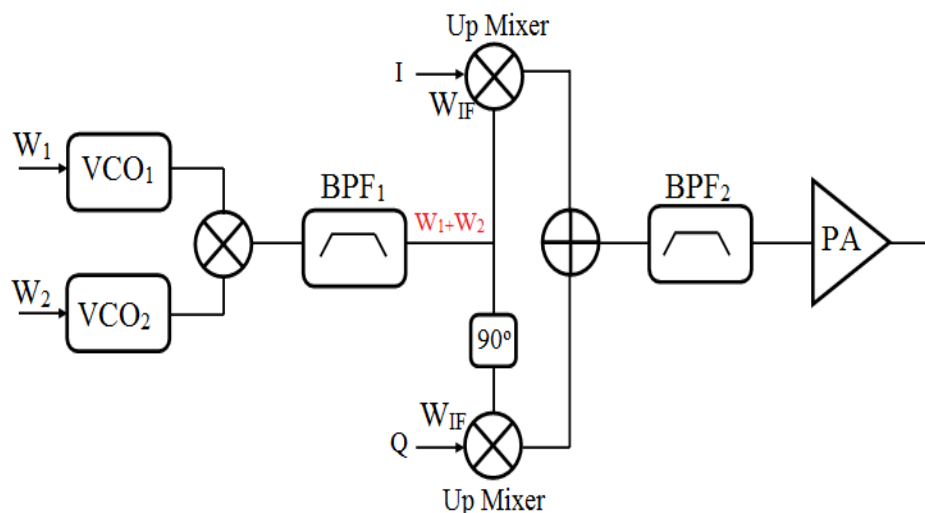

Figure 3. Offset direct conversion transmitter configuration.

- Direct modulation
  This transmitter architecture which is shown in Figure 4 [30] works for phase and frequency modulations with a simple configuration. This transmitter is power efficient and provides a good integration. When signals are transmitted, voltage

controlled oscillator frequency instabilities can occur and need to be considered carefully [30].
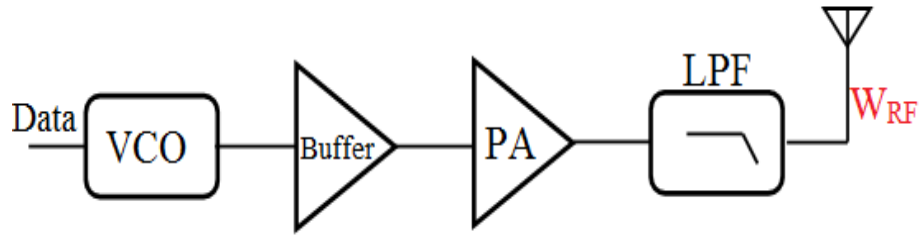

Figure 4. Direct modulation transmitter configuration.

Receiver removes the radio frequency carrier from the received signal and amplifies that signal to an appropriate level needed to enter the ADC. Receiver is responsible for demodulation of an intended signal in the presence of interferes and noise. At the receiver side, the RF signal is reinforced again since a strong attenuation has suppressed the transfered signal during the signal path. Different receiver architectures are compared in Table 2 [30]. Selecting a desirable architecture depends on the available technologies and required specifications in the receiver design. Among these architectures digital- intermediate frequency (IF) and low-IF receivers have flexible architecture and good performance respectively [30]. Here different architectures mentioned in Table 2, are examined.

Table 2. Specifications of different receiver architectures

Architecture	Complexity	Power Consumption
Superheterodyne	Moderate	Moderate
Dual superheterodyne	High	High
Direct conversion	Low	Low
Impulse radio	Low	Very low
Low-IF	Moderate	Moderate
Digital-IF	Very low for RF, very high for baseband	Very high

- Superheterodyne
  Superheterodyne receivers are modeled as down conversion or up conversion receivers. Superheterodyne receivers have several benefits such as good dynamic range and a good sensitivity since the amplification is done on several frequencies. Superheterodyne receiver structure is shown in Figure 5 [30].
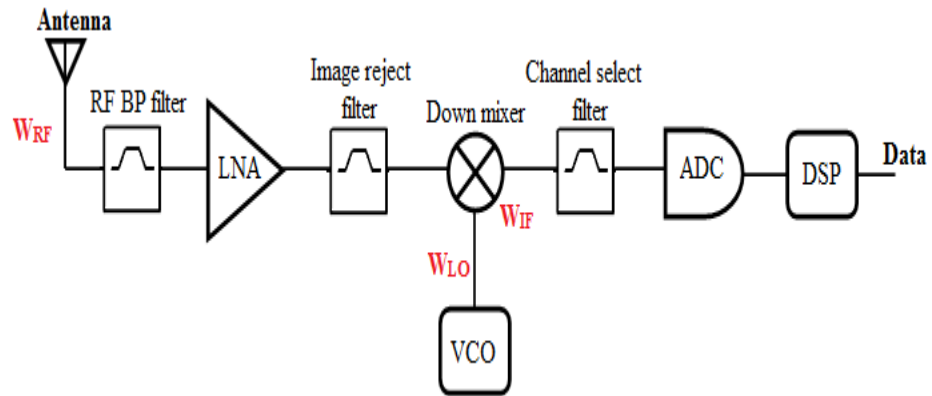
Figure 5. Superheterodyne receiver configuration.

- Direct conversion

  This architecture that is presented in Figure 6 [30] is also popular as homodyne or zero-IF conversion. This kind of receiver which is indicated in Figure 6 utilizes low pass filters in order to separate the desired signal from the interference signal and straightly converts the RF to the BB signal which has made the digital signal processing easier [32]. This architecture has several benefits in comparison with superheterodyne receivers such as simple architecture, no image frequency problem, less spurious responses and integration is done more easily [30].
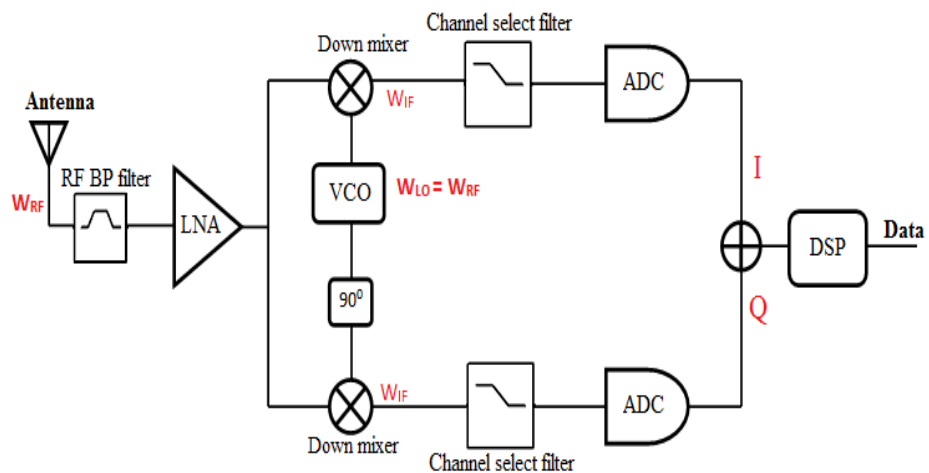

Figure 6. Direct conversion receiver configuration.

- Low-IF

  Low-IF architectures are employed in order to eliminate some problems such as LO leakage and flicker noise in direct conversion receivers. In low-IF receivers, an RF signal is converted to non-zero low intermediate frequency. IF is chosen in a way that its value is about one or two times of the channel bandwidth [32].

- Digital-IF

  A high speed ADC is used after converting the RF signal to the IF one to have

a digital data stream which goes into the next processing stages and provides a flexible system. Moreover, digital-IF receivers do not face magnitude and phase mismatch problems [30]. Structure of the digital-IF receiver is illustrated in Figure 7 [30].
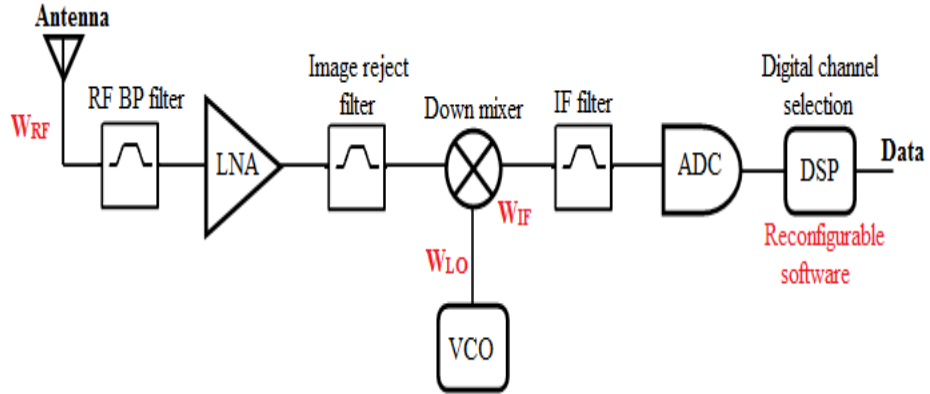

Figure 7. Digital-IF receiver configuration.

2.3. Full Duplex Transceivers Impairments

A typical full duplex transceiver utilized in several literatures is shown in Figure 8 [33] provides an isolation between TX and RX through two separate antennas. This architecture is attractive due to the easy and extensive application of direct-conversion architecture [33]. As we mentioned earlier in the introduction, the important challenge in full duplex transceiver design is combating the self-interference signal due to the employing a shared antenna between transmitter and receiver or using two separate antennas located close to each other [8]. Different factors which are not considered as a part of cancellation process, limit the amount of SI suppression in FD systems such as RF components nonidealities, phase noise and IQ imaging, nonlinear distortions due to the amplifiers and mixers and also quantization noise [8], [34].

In this model, first a digital baseband (BB) signal is generated when data streams are entered into the coder and then modulated. Then it is converted into the analog signal which passes through a low pass filter and then converts to a higher carrier frequency and eventually amplified before being transmitted via the antenna. Received signal in the same frequency band is passed through a bandpass filter and low noise amplifier before being converted to BB frequency. Afterwards, signal is processed by a low pass filter (LPF) and a variable gain amplifier (VGA) and finally converted to the digital signal in order to be processed by a decoder.

In this architecture, the interference signal is transmitted directly from the transmitter antenna into the receiver antenna in a full duplex system when separate antennas are employed.

In the following sections different transceiver impairments mentioned earlier are examined in more details.
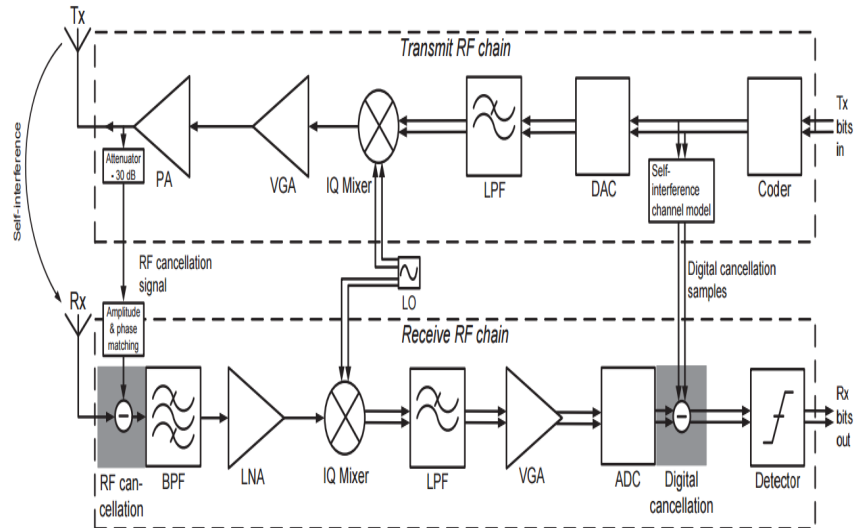
Figure 8. Structure of full duplex direct conversion transceiver.

2.3.1. Phase Noise

In the transmitter configuration the oscillator is used to produce a carrier signal needed for up conversion process of baseband signal. Phase noise is a considerable problem in oscillators which affects the performance of the system, noise floor and bit error rate in case of having phase modulation. Phase noise is created through the up conversion and down conversion at the transmitter and receiver sides respectively [34]. So we have

$$\hat{x} = \Re[\tilde{x}e^{j(2\pi f_c t + \phi_{TX}(t))}], \tag{1}$$

$$\hat{r} = LPF[\hat{x}e^{-j(2\pi f_c t + \phi_{RX}(t-\Delta t))}], \tag{2}$$

where $\hat{x}$ and $\tilde{x}$ refer to the amplified up converted analog signal and the analog BB signal. $\hat{r}$ is the down converted signal at the receiver, $\phi_{TX}(t)$ and $\phi_{RX}(t)$ are representative of the phase noise process of oscillator at the transmitter and at the receiver sides respectively. Simple delay due to the SI channel is also shown by $\delta(t - \Delta t)$.

Low pass filter (LPF) is used in order to eliminate unwanted signals around $\pm 2f_c$. In full duplex systems a common oscillator is considered in the transceiver design which leads to the equal phase noise process of the oscillator at the transmitter and receiver and also can be defined only with $\phi(t)$ while in systems with separate oscillators, phase noise process of transmitter and receiver are uncorrelated [34]. Phase noise effect of oscillators in radio transceivers are examined in [35], [36] and authors in [24] have analyzed its impact on the system efficiency under the asynchronous FD wireless communications.

2.3.2. Nonlinear Distortions

Nonlinear distortions are generated by components used in radio circuits. If x is the input signal, nonlinear distortions can be expressed by Taylor series as follow [34]

$$\hat{x} = \sum_{n=1}^{n_{max}} \beta_n x^n \;\;, \; where \; \beta_n \in \mathbb{R}. \tag{3}$$

$IIP2$ (second order of input intercept point) and $IIP3$ (third order of input intercept point) are used to characterize the nonlinear distortions when amplifiers operate in a nonlinear region or produce intermodulation products of the input signals [8]. Nonlinear distortions deteriorate the system performance.

Nonlinear distortions generated by LNA, mixers and variable gain amplifier at the receiver are calculated by input intercept points (IIP_n) as follow

$$P_{nth} = P_{out} - (n-1)(IIPn - P_{in}), \tag{4}$$

where P_{in} and P_{out} are total input and output powers respectively in dBm [8] . In [8] these equations are discussed in more details. Moreover, in the transmitter chain, power amplifier plays a significant role in producing the nonlinear distortions since distortions which are generated by other components are eliminated through the RF cancellation. On the other hand, nonlinear distortions of the transmitter are a big concern in the full duplex transceivers since analog distortions are not considered in the reference cancellation signal taken for the digital cancellation process; hence, this kind of distortions are not canceled through the linear digital cancellation [8], [33]. Moreover, in literatures such as [33] and [17], authors have examined techniques to mitigate the nonlinear distortions in digital domain which improves the total SIC. Nonlinear distortions can be minimized through using more linear components in the transceiver design but it would be highly costly in full duplex transceivers [37].

2.3.3. Quantization Noise

One of the momentous issues in FD transceiver design is the dynamic range of ADC. In order to occupy the entire available dynamic area of ADC, signal at the receiver chain is amplified by a VGA while under a severe self-interference signal the amount of employed dynamic range of ADC and consequently resolution of the signal decreases considerably since some amount of the dynamic range of ADC is occupied by the residual unwanted signal [38], [8]. There are various techniques to overcome the impact of quantization noise. For example, one way is improving the resolution of the intended signal by adding more bits to the ADC in case of having a severe self-interference signal [37]. For instance, the dynamic range of an analog-to-digital converter improves almost 6 dB by increasing one bit [8]. Another way would be suppressing the level of self-interference signal prior to entering the analog-to-digital converter through considering another analog SIC at the baseband phase or boosting the RF suppression efficiency [37]. Power of the quantization noise at the input of the detector can be calculated by [8], [37]

$$P_{quant} = P_{target} - SNR_{ADC} = P_{target} - 6.02b - 1.76 + PAPR, \qquad (5)$$

where $PAPR$ is the peak-to-average power ratio, P_{target} is the total power at the input of ADC, SNR_{ADC} is signal-to-quantization-noise ratio and b is the number of bits at the ADC. Dynamic range of one bit is indicated by 6.02 [8], [37], [39].

2.3.4. Thermal Noise

Thermal noise induced by the transmitter is another RF impairment in a FD radio transceiver which is not discussed in many literatures. Thermal noise in the transmitter chain is intensified through passing the transmitter's components such as the mixer, variable gain amplifier and power amplifier in case of having an ideal low pass filter while its value is at the level of the thermal noise floor after the digital-to-analog converter (DAC) [37]. Authors in [37] provide more information regarding the impact of thermal noise induced by transmitter and they have taken into account this issue in their simulations.

2.4. Self-interference Cancellation in Full Duplex Systems

Self-interference cancellation is done in passive and active domains. A proper full duplex communication is possible through employing both domains in a SIC process since a passive cancellation provides insufficient amount of required SIC. Active cancellation involves analog and digital cancellation techniques which are discussed in more details in the following sections. All in all, cancellation can be done in four phases to provide a desirable full duplex communication [33] which are shown in Figure 9 [27] in terms of power levels. The first two phases can be considered as alternative solutions.

- Providing a good isolation between two antennas or the circulator in case of separate antennas and a shared antenna respectively which refers to the passive SIC.

- Performing active SIC for a full duplex system with multi-antenna case through the beamforming.

- Taking the transmit signal as the cancellation signal for analog suppression in baseband frequency or RF domain.

- The amount of SI signal which is left, can be mitigated via the digital suppression technique.
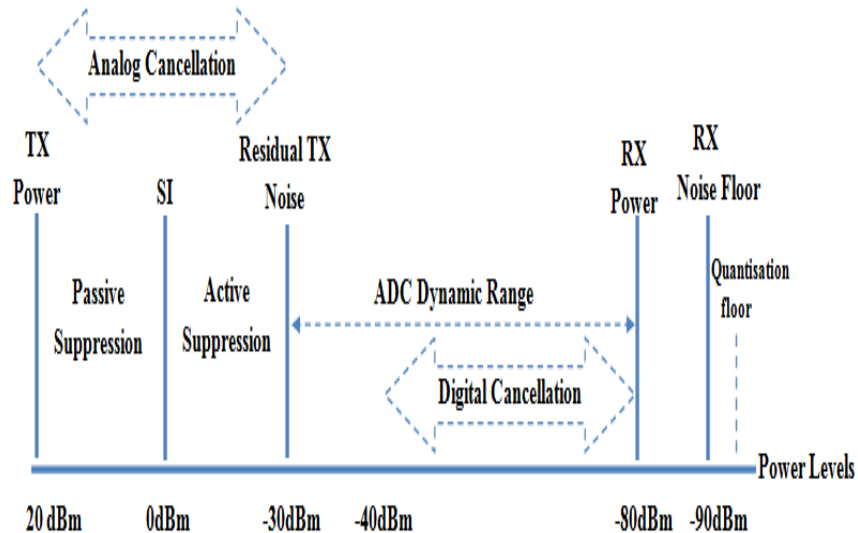
Figure 9. Distributed power levels for a full duplex transceiver according to different phases of cancellation in analog and digital domains.

2.4.1. Connection between SIC and FD Transceiver Efficiency

The level of SIC that the transceiver attains, determines the performance limitations of the system. In order to understand the connection between SIC and FD transceiver specifications, we can define the power levels of the receiver and remained SI signal according to the P_R, P_T, P_{RSI} and $SSINR$ which are representative of power levels related to the intended received signal, transmitted signal, residual self-interference signal and signal-to-self-interference-plus-noise-ratio respectively [40].

$$P_{R(dBm)} = P_{T(dBm)} - Path\ loss_{(dB)}, \tag{6}$$

$$P_{RSI(dBm)} = P_{T(dBm)} - SIC_{(dB)}, \tag{7}$$

$$SSINR_{(dB)} = P_{R(dBm)} - P_{RSI(dBm)}. \tag{8}$$

If both nodes transmit at the same power equation (8) is equal to

$$SSINR_{(dB)} = SIC_{(dB)} - Path\ loss_{(dB)}. \tag{9}$$

For having a good FD system, transceiver has to suppress the unwanted signal to the below of the noise floor at the RX [40], [41]. Transmitter noise is one of the major factors which restricts the performance of active SIC since in active cancellation technique, transmitter noise is not characterized in the BB as it has a random value [40]. In order to remove the transmitter noise, analog noise suppression technique takes a replica of the noise from its generation point and performs the cancellation process in that point as well [17]. Authors in [22] have canceled the noise through employing a cancellation circuit.

The relationship between the power levels in equations (6-8) can be illustrated based on the full scale (FS) parameter [40]. FS is what determines the upper bound for the P_R. In Figure 10 [40], signal-to-noise-ratio of the receiver is displayed by SNR_R and $SSINR$ refers to the signal-to-noise-ratio of a full duplex radio transceiver.
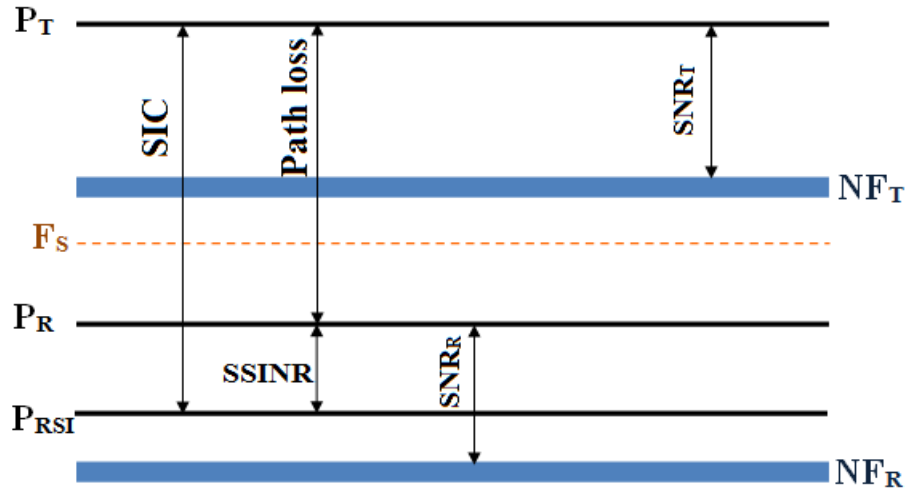

Figure 10. Distribution of power levels in a full duplex system and the level of self-interference suppression.

2.4.2. Active Analog Cancellation

In radio communications, some amount of the transmitted signal leaks to the receiver due to the simultaneous transmission and reception which corrupts the intended signal at the receiver. It is desirable to eliminate a large amount of interference signal before ADC. Active analog cancellation technique is performed after receiving the transmitted signal. Here two different architectures of analog cancellation which are different based on where the reference signal is selected, are discussed briefly.

- Stanford architecture (Post mixer canceler)
  The cancellation signal is generated by attenuation and phase inversion of the RF transmitted signal prior to entering the LNA at the receiver chain. This method is beneficial as the cancellation signal contains hardware deficiencies of the transmitter chain as well. Applying a digital cancellation technique after an analog RF cancellation improves the efficiency of Stanford architecture but it is not suitable for systems with multiple antennas since costly and complicated analog circuits are needed [17], [34]. Stanford configuration and its analog canceler are presented in Figure 11 [42] and Figure 12 [17] respectively.
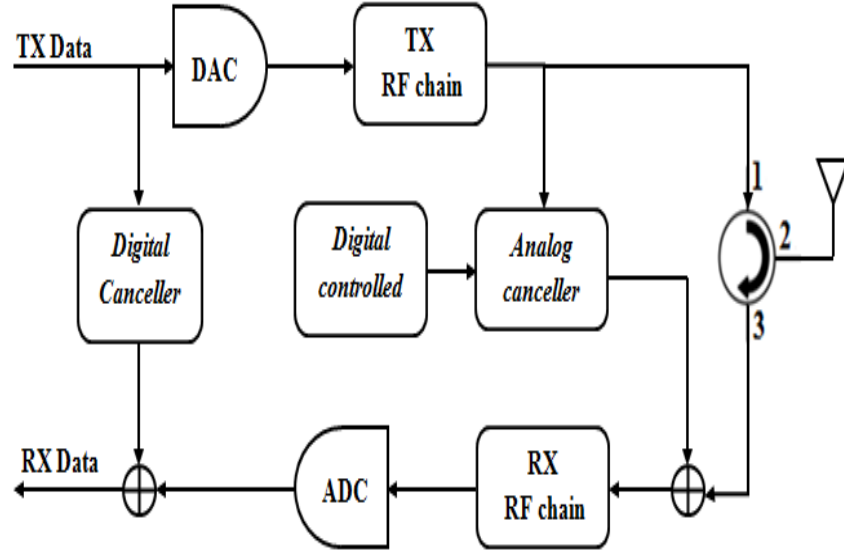
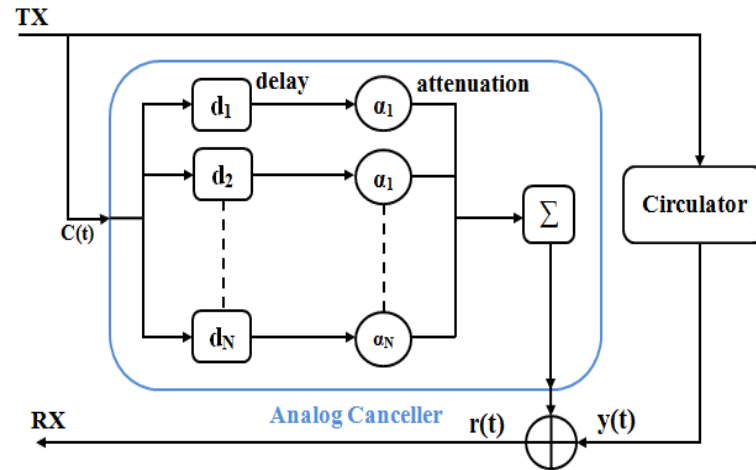Figure 11. Stanford architecture with RF active cancellation.

Figure 12. Analog canceler of active cancellation utilized in Stanford architecture.

According to the Figure 12, where $r(t)$, $c(t)$ and $y(t)$ are the received signal, transmit coupled signal and the unwanted signal respectively, we should find the attenuation value α and delay time d in such a way that the unwanted signal is minimized. We can write the cost function as

$$r(t) = y(t) - \sum_{i=1}^{N} \alpha_i c(t - d_i). \tag{10}$$

The cost function equation in frequency domain is calculated by

$$R(f) = Y(f) - \sum_{i=1}^{N} H_i^{\alpha_i}(f) C(f), \tag{11}$$

where $Y(f) = H(f)C(f)$ and $H_i^{\alpha_i}(f) = \alpha_i e^{(j2\pi f d_i)}$. $H(f)$ and $C(f)$ represent the self-interference channel and the reference signal in frequency domain respectively [17]. The analog canceler is defined by calculating the minimum value of the optimization problem.

$$min_{\alpha_1,...,\alpha_N} \ (H(f) - \sum_{i=1}^{N} H_i^{\alpha_i}(f))^2. \qquad (12)$$

Equation (12) is solved in two phases. We need to find the frequency response of the SI channel $H(f)$ and each delay applied to the reference signal per each attenuation value $H_i^{\alpha_i}(f)$. In this case, we attain all possible combinations of attenuation and delay values in order to determine the best required combination for the analog canceller to suppress the self-interference signal [17].

- Rice architecture (Pre-mixer canceller)
  Rice architecture which is indicated in Figure 13 [42] utilizes a delayed and attenuated baseband signal through an auxiliary radio chain to suppress the self-interference signal. This techniques is not able to eliminate the transmitter impairments such as phase noise and nonlinearities and provides small amount of digital cancellation [34], [43]. Different Rice architectures are examined in [43], [44].
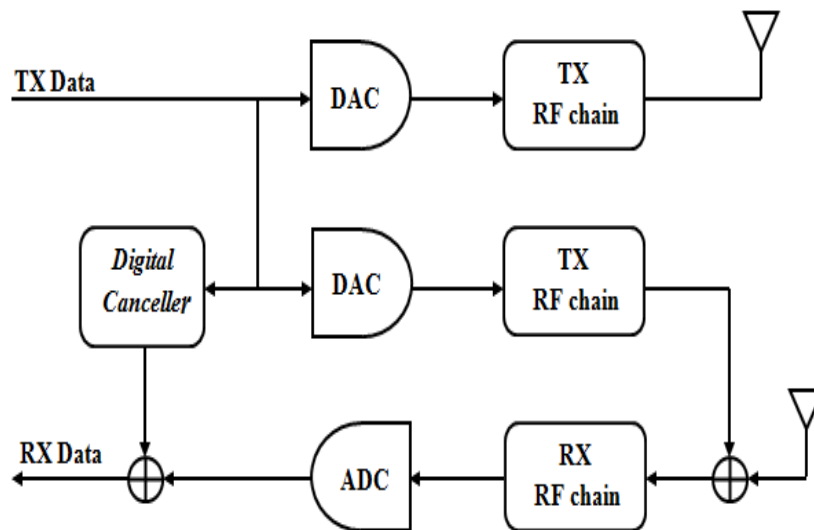

Figure 13. Rice architecture with baseband active cancellation.

2.4.3. Passive Analog Cancellation

Passive analog SI cancellation is done based on the antenna separation through decreasing power of the propagated electromagnetic signal with separated TX/RX antennas or based on the antenna cancellation (or null positioning) technique. In this case,

TX/RX antennas are located symmetrical with π-phase shift (refered as NEC architecture) or can be placed asymmetrical. In asymmetrical case, half of the wavelength is considered to balance transmitters in a way that their signals are added destructively which leads to a null position and a weaker signal arrives at the receiver [45]. Both conditions are displayed in Figure 14 [45].
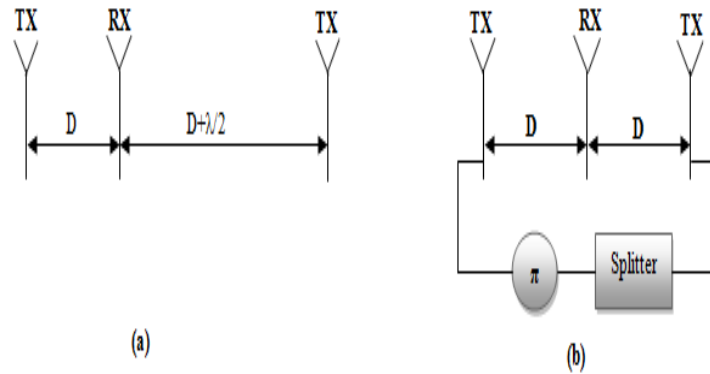

Figure 14. Antenna cancellation techniques for a) asymmetrical b) symmetrical distances.

The other approach is using a passive device called circulator with three or four ports. When a radio frequency signal enters any port of a circulator, signal is rotated and forwarded to the next port. Circulators are considered as a type of duplexer which rotates the signal from the transmitter to the antenna and then from the antenna to the receiver without any direct leakage from the transmitter to the receiver. All in all, if the amount of passive self-interference cancellation increases, the wireless systems behave more frequency selective and its amount is restricted by the environmental reflections [17].

An RF circulator is a 3-port ferromagnetic device which controls the signal transmission between two ports while provides an isolation from the third port. Selecting a desirable circulator depends on several specification as follows [46]

- Frequency range
  This is important to determine the frequency range of operation since we aim to have the minimum insertion loss.

- Insertion loss
  This parameter is defined as the difference between power of the incident signal at one port and the arrived signal at the next port. Its value is measured in dB.

- Isolation
  Isolation value shows how perfect the circulator works. Its value is measured between adjacent ports of the circulator and depends on the amount of insertion loss.

- Power
  This is important to know the power threshold of the circulator needed to perform properly.

2.4.4. Digital Cancellation

Employing both analog and digital cancellation techniques provide a high isolation between the transmitter and the receiver so the cancellation process can be continued by digital suppression method to eliminate the unwanted signal which is left in the received signal [34]. In digital suppression we need to estimate function of the complex baseband SI signal in order to subtract it from the received signal [34]. Complex received signal r at the baseband is calculated by equation (13) where x, z and s are complex baseband SI signal, noise and intended signal respectively.

$$r = f(x) + z + s. \tag{13}$$

- Linear Digital Cancellation
  In linear digital cancellation, the least square (LS) algorithm is utilized in order to estimate the self-interference channel H_{SI}. Equation (13) can be simplified as [34]

$$r = H_{SI} * x + z + s, \tag{14}$$

$$r - \hat{r} = H_{SI} * x - \hat{H}_{SI} * x + z + s. \tag{15}$$

  Function of signal x is changed to the convolution of the self-interference channel and the baseband self-interference signal. Equation (15) represents the linear digital cancellation term, where $\hat{r}$ and $\hat{H}_{SI}$ are the least square estimates of the received complex BB signal and the self-interference channel respectively and z represents the total noise [34].

- Nonlinear Digital Cancellation
  On the other hand, PA generates nonlinearities which leads to the transceivers impairments. As mentioned earlier in Section 2.3.2 nonlinear distortions are expressed by Taylor series. Equation (13) is changed to the equation (16) where n is considered as baseband signal odd harmonics and $H_{SI,n}$ is the SI channel related to each harmonics of the BB signal estimated by LS estimator. In equation (16) n_{max} is the maximum harmonics allocated to the baseband signal [34].

$$r = \sum_{n=1,n \ odd}^{n_{max}} H_{SI,n} * x^n + s + z. \tag{16}$$

Majority of suppression techniques can be utilized at low powers with a desirable performance since the non-idealities are mostly under the thermal noise floor and less amount of cancellation needs to be considered. On the other hand, if the amount of analog suppression increases, less amount of digital cancellation is needed since the residual self-interference signal diminishes. Moreover, hardware impairments of full duplex transceivers restrict the amount of accessible SIC [34].

2.5. Summary

This chapter discusses the full duplex technology concept and the challenges in FD implementation. Full duplex approach provides various benefits in comparison with half duplex (FDD or TDD) techniques. Canceling an unwanted signal (called self-interference signal) which leaks from the transmitter to the receiver is a big challenge in FD systems. In recent years, several research groups have studied different methods to suppress that unwanted signal in digital and analog domains of a transceiver chain. Removing the self-inference signal leads to a better system throughput and improving the spectral efficiency to almost two times of a conventional frequency division duplex system.

3. ELECTRICAL BALANCE DUPLEXER

In this chapter the electrical balance duplexer as the first SIC technique in this thesis is studied. Structure, components and its performance are investigated. An electrical balance duplexer consists of a hybrid transformer and a balancing network which are discussed in more details in the following sections.

3.1. Electrical Balance Duplexer

Electrical balance duplexers perform in a way to provide impedance matching between the antenna and the balance network at the ports of the utilized hybrid transformer to suppress the signal transmission from transmitter to receiver. In other words, to provide a high isolation between TX and RX ports [47], [48]. Electrical balance duplexer can be used in both FDD (through utilized hybrid transformer) and FD techniques. Structure of an electrical balance duplexer is displayed in Figure 15 [49].
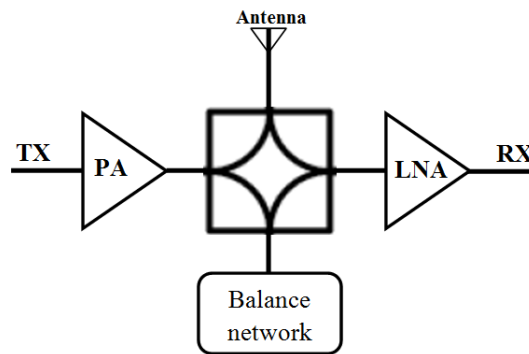
Figure 15. Tunable electrical balance duplexer.

3.2. Transformer

In this section we study the hybrid transformer and specifications of an ideal hybrid transformer are also discussed. Moreover, the relation between transformer ports and the isolation conditions are demonstrated.

3.2.1. Hybrid Transformer

For a long period, hybrid transformers were used in the telephone handsets in order to provide an isolation between microphone and earphone and reduce the sidetone [50], [51]. According to the two main capabilities of hybrid transformers, impedance matching and conjugation between ports, signals from different ports can be separated or mixed without any interaction [50]. A hybrid transformer illustrated in Figure 16 [49] consists of four ports (W, X, Z, Y) which are connected to TX, antenna, balance network and RX respectively and it can be considered as a return-loss bridge. In an ideal

hybrid transformer, there is an impedance matching between antenna and balance network; therefore, the power from PA at the TX port is divided equally between the antenna and the balance network; hence, no power goes to the opposite branch and the ports W and Y are conjugated ports. In this case a high isolation is attained between TX-to-RX ports.
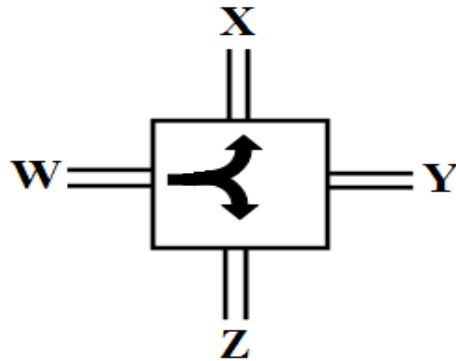

Figure 16. Schematic diagram of a hybrid transformer.

Ideal hybrid transformers have four prevalent features as follows

- Bi-conjugacy
  As discussed earlier, in a conjugate case, no power transfers from port W to port Y only if the impedance of ports X and Z are equal; hence, W and Y are called conjugate ports. Moreover, ports X and Z also could be conjugated only if a good termination exists at ports W and Y as well [50].

- 180° phase shift
  In transformer design, we should note that apart from the transformer configuration, there is a 180° phase inversion in one of the transmission ratios [49]. This feature is shown in Figure 17 [49].
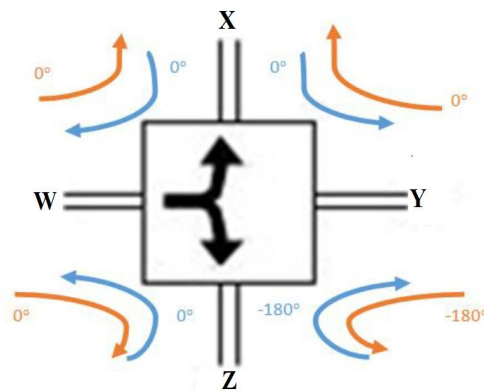

Figure 17. 180° phase inversion in signal transmission through hybrid transformer.
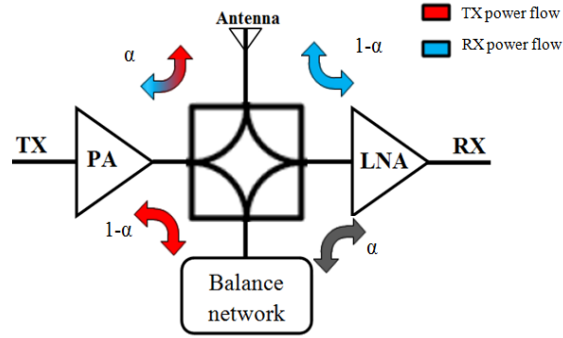
- Power splitting

Figure 18. Power ratios between ports of a hybrid transformer.

Hybrid transformers give the designer the opportunity to determine desirable power ratio (γ) between different ports. According to the Figure 18 [49] we have [49]

$$\gamma = \frac{P_{ANT}}{P_{BAL}} = \sqrt{\frac{\alpha}{(1-\alpha)}}, \tag{17}$$

$$\frac{P_{ANT}}{P_{RX}} = \frac{\gamma}{\gamma + 1}, \tag{18}$$

$$\frac{P_{BAL}}{P_{RX}} = \frac{1}{\gamma + 1}, \tag{19}$$

where P_{RX} is the power of the receiver which is equal to $P_{ANT} + P_{BAL}$. Power of the antenna and power of the balance network are displayed by P_{ANT} and P_{BAL} respectively.

- Impedance matching
  If the transformer is center tapped and balanced ($\gamma = 1$), antenna and balance ports have equal powers and $Z_{BAL} = Z_{ANT} = 2Z_{TX} = Z_{RX}/2$; otherwise, $Z_{BAL} = \gamma \times Z_{ANT} = (1 + \gamma)Z_{TX} = (\gamma/1 + \gamma)Z_{RX}$.

In case of impedance matching and conjugacy in Figure 19, impedances Z_1, Z_2, Z_3, Z_4 have the following relations [50].

$$Z_2 = Z_3, \tag{20}$$

$$Z_4 = Z_3/2, \tag{21}$$

$$Z_1 = (N_2/N_1)^2 \times (Z_3/2). \tag{22}$$

Authors in [51] have discussed about the hybrid transformer, connection between ports through power gain and available gain at each ports in more details. They have presented that the amount of power which is transfered from the TX port to the ANT port when $Z_{TX} \neq Z_{ANT}$ is determined by a ratio called transducer power gain (g_{tr}) which is equal to the amount of power received at the antenna port to the amount of power existent at the transmitter side [51]. The relationships between the hybrid transformer

ports according to Figure 16 [49] are illustrated in the Table 3 [50] and an ideal hybrid transformer is indicated in Figure 19 [50].

Table 3. Connections between hybrid transformer ports

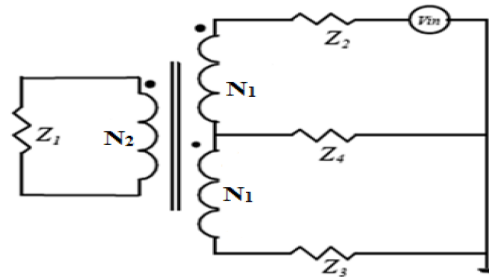| Transmitting port	Power ratio	Conjugate port
W	Port X/Port Z	Y
X	Port W/Port Y	Z
Z	Port W/Port Y	X
Y	Port X/Port Z	W

Figure 19. Ideal hybrid transformer model.

3.3. Balancing Network

The balance network is an essential part of an electrical balance duplexer. It performs linearly and supports an appropriate tuning range of impedances [2]. Balance network is required to provide isolation between the transmitter and the receiver. In this case its impedance should be equal to the antenna impedance. In order to support a wide scope of isolation bandwidth (BW), four tunable capacitors are used in the balance circuit structure to enable the impedance matching at the operating frequency according to the real and imaginary parts of the impedances [2], [52]. The optimization of these four capacitors is done concurrently on a common frequency and in case of having a FDD system we should considers both TX and RX frequencies for isolation. This is due to the fact that tuning the balance network impedance at the TX and RX frequencies independently is not feasible since these impedances are not independent of each other and changing in any of these impedances will affect the other one [2]. Two inductors and a resistor are also used in this circuit. The criteria of choosing the values for the inductors is minimizing the capacitance tuning ratio required to cover the desirable area of impedance on the Smith chart in addition to being equal [2]. Here only two inductors are employed due to the limitation of the execution space. The resistor is used to share the power between the antenna and the balance network [52]. Structure of the balance network is indicated in Figure 20 [52].
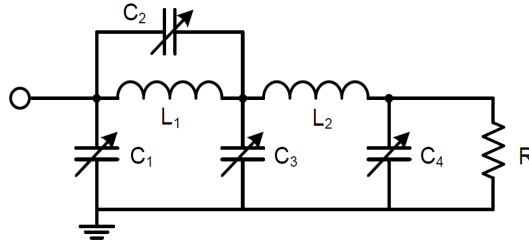
Figure 20. Balance network schematic.

3.3.1. Balancing Region and Balancing Resolution

The scope of impedance in which the balancing circuit can cover at a certain frequency is determined by the balancing region. As we mentioned earlier, in order to have a good isolation between the TX and RX, the balance network needs to follow the impedance variations of the antenna. Therefore, to find out a precise copy of the impedance at the antenna port, a high grade of resolution is needed. Since the impedance value consists of both imaginary and real parts, a good resolution arrives by tuning both parts in a complex impedance plane [49].

3.3.2. Isolation and Isolation Bandwidth

According to the Figure 21 [49] the required isolation in an electrical balance duplexer with ideal elements under a good symmetry is calculated by equation (23) where $Z_{ind,p}$ and V_x are the self-inductance and the center tap swing voltage of the employed transformer [49].

$$Isolation_{TX} = -20\log_{10}(|Z_{ANT} - Z_{BAL}||\frac{Z_{ind,p}}{(Z_{ANT} + Z_{ind,p})(Z_{BAL} + Z_{ind,p})}| \times V_x).$$
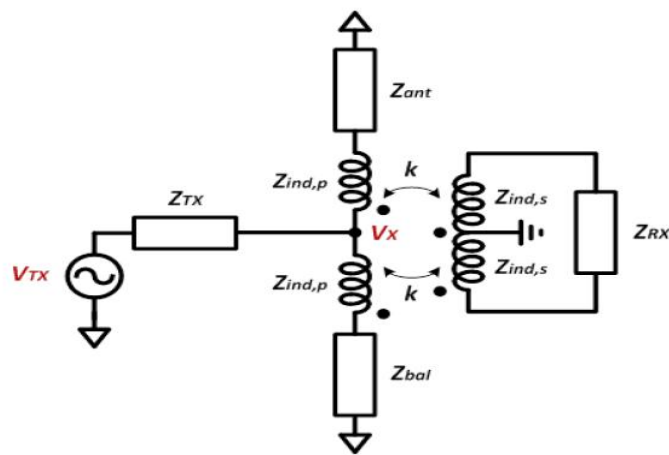
(23)

Figure 21. Isolation in an electrical balance duplexer according to the antenna impedance and balance network impedance.

According to the equation (23), the antenna impedance Z_{ANT} is surrounded with a circle of radius equal to the term $|Z_{ANT} - Z_{BAL}|$ which indicates that all available impedances with a specific distance away from the antenna impedance, bring almost the same isolation value. On the other hand, $|Z_{ANT} - Z_{BAL}| = 0.5$ refers to 6 dB growth in the isolation value [49].

The frequency scope in which the determined isolation value is attained refers to the isolation bandwidth [49]. Range of the isolation bandwidth depends on the balance network. According to the Figure 20 through tuning the tunable components, the balance network is able to follow the antenna impedance variations in order to detect a compromise between the frequency range and the average isolation [52]. The relationship between the isolation, antenna impedance and impedance of the balance circuit is defined as [49]

$$Isolation_{TX}(w) \propto -20 \log_{10}(|Z_{ANT}(w) - Z_{BAL}(w)|). \tag{24}$$

$Isolation_{TX}(w)$, $Z_{ANT}(w)$ and $Z_{BAL}(w)$ are the isolation, antenna impedance and the balance network impedance across the bandwidth.

3.3.3. Necessity of the Linear Behavior in the Balance Network

Nonlinearity of the balance network leads to the generation of the intermodulation products which are then coupled to the input of the low noise amplifier and result in 3 dB loss in the power. Consequently the isolation decreases. The balance network performs satisfactory, if the level of the essential components entered into the LNA is higher than the distortions such as third-order intermodulation ($IM3$) [2].

$$IM3_{BAL}(dBm) - 3\ dB < P_{TX}(dBm) - 3\ dB - ISOL_{TX-RX}(dB). \tag{25}$$

According to the Figure 22 [2], equation (25) shows the linearity requirement of a balance network which holds if fully passive components and extremely linear tunable capacitors in the structure of the balance network are employed [2].

Moreover, the third-order input intercept point ($IIP3$) can be defined according to the transmitter power and the amount of TX-to-RX isolation as

$$IIP3_{BAL}(dBm) = \frac{3}{2}(P_{TX}(dBm) - 6\ dB) - \frac{1}{2}IM3_{BAL}(dBm), \tag{26}$$

$$IIP3_{BAL}(dBm) > P_{TX}(dBm) + \frac{1}{2}ISOL_{TX-RX}(dB) - 9\ dB. \tag{27}$$
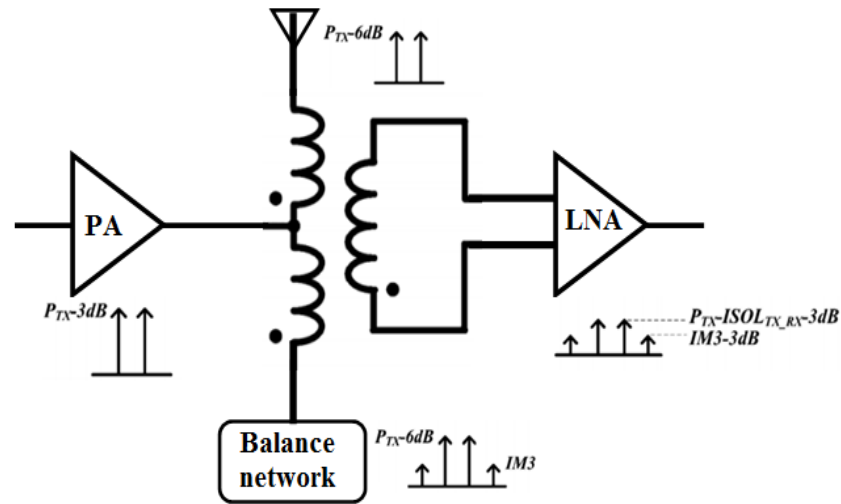
Figure 22. Coupled nonlinear distortions to the input of LNA.

3.4. Tracking Loop

The amount of the signal transfered from the transmitter to the receiver side can be minimized through a tracking loop. Tracking loops are used to follow the transmission continuously and detect the magnitude of the transmitter leakage. Then a correction command is sent back to the bridge balance in order to tune the impedance between the antenna and the balance ports of the hybrid transformer. This process is performed by employing a local oscillator (LO) [2].

3.5. Tuning Algorithm

The impedance of the antenna changes as a result of the communication environment variations. Authors in [1] have studied an algorithm in order to tune the impedance and maintain the matching impedance between the antenna and the balance network during the communication. They have shown that the balance network impedance is tuned based on the enlargement of $\Delta\Gamma$ which is equal to $\Delta\Gamma_{ant}$ - $\Delta\Gamma_{Balance}$. Since the antenna impedance does not remain constant during the radio communications, phase of $\Delta\Gamma$ is also needed to keep the matching impedance between the antenna and the balance circuit. The required phase is determined based on an algorithm called "Angular search algorithm" which is shown in Figure 23 [1]. In this algorithm, amplitude of $\Delta\Gamma$ remains constant while the phase of $\Delta\Gamma$ varies and the level of cancellation related to each phase shift is measured in order to find out the optimal value of phase [1]. In [1] it is presented that a greater level of self-interference suppression is provided by those phases close to the maximum value of SIC compared to the other phases which are far away from the maximum value of SIC. All in all, the tuning algorithm can be defined as follow
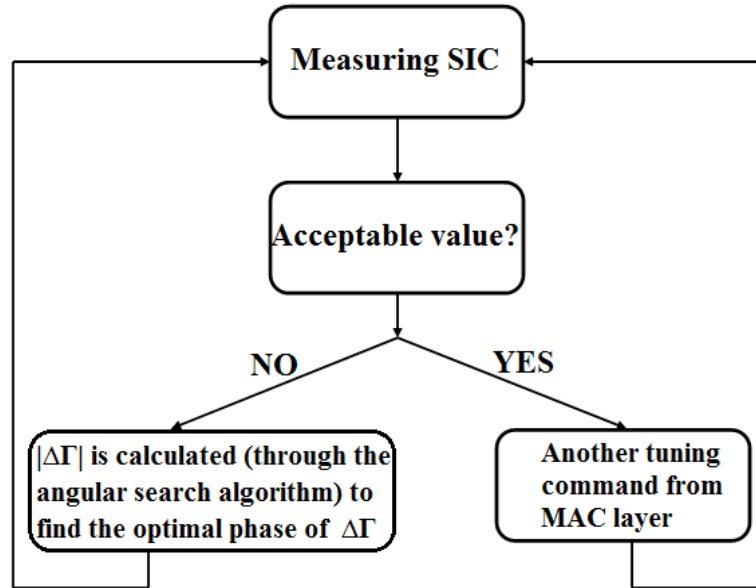
Figure 23. Angular search algorithm process.

3.6. Recent SIC Techniques with EBD

Table 4 represents recent self-interference cancellation techniques which have utilized electrical balance duplexer. Total level of isolation and operation bandwidth of each method is also indicated here.

Table 4. Related RF SIC techniques with EBD

$Reference$	Isolation	Bandwidth
[53]	50 dB	$1.6 - 2.2$ GHz
[1]	50 dB	20 MHz
[54]	> 50 dB	$1.5 - 2.5$ GHz
[52]	55 dB	138 MHz
[55]	50 dB	6 MHZ

Authors in [52] have considered a $50\ \Omega$ impedance as an alternative to a real antenna and in [1] a tuning algorithm is applied to achieve 50 dB total SIC.

3.7. Summary

This chapter shows the electrical balance duplexer structure as an RF SIC technique. Electrical balance duplexer can be used when a single antenna is shared between the transmitter and the receiver while we need to keep the isolation between the TX and RX ports in RF domain. The important features of the balance network and the relationship between the antenna impedance and the balance network impedance needed to provide TX-to-RX isolation are discussed clearly. Finding the optimal values for the tunable components of the balance network in order to follow the antenna impedance variations

is the main concern in this approach. Some related SIC techniques worked with EBD are also mentioned at the end of this chapter.

4. RF SELF-INTERFERENCE SUPPRESSION

This chapter examines the second technique of RF self-interference suppression based on the antenna prototype. Two options are proposed for RF SIC through the antenna. One technique is providing the isolation between ports of a dual-feed antenna and the other one would be utilizing two separate antennas with a specific distance from each other but due to the surface limitation in radio communication apparatuses, it is not possible to use convoluted antennas. This chapter describes FD structure based on the separate TX and RX antennas, and a dual feed antenna. Moreover, polarization of the antenna is discussed briefly since the isolation value depends on the polarization of antenna as well.

4.1. Active Analog Cancellation Topologies

The amount of the interferer signal which enters the RX side, varies as a result of variations in a real communication environment such as impact of the human body on the antenna impedance. In order to reduce the effect of the environment variations on the antenna performance, an active cancellation is employed between the antenna ports [52]. There are different topologies to employ the active cancellation which are discussed in the following sections. In this thesis we focus on the active analog cancellation with a dual polarized antenna which is discussed in Section 4.1.2.

4.1.1. Front-end Model with Separate Antennas

In an RF front end the electromagnetic signal passes through the filters, amplifiers and mixers since transmitting the baseband signal directly via the channels is impractical. In this architecture two separate antennas are considered for transmission and reception.

Figure 24 [52] represents that a copy of the amplified up converted signal is taken and passed through an attenuator which works in such way that the level of the attenuation is specified regarding the amount of the isolation provided by the antennas. Attenuated signal is then phase shifted prior to passing through the down converter. SIC takes place by deducting this manipulated signal from the received analog signal. In this architecture there is a possibility of having down converter prior to the LNA which simplifies the architecture since attenuation, phase inversion and down conversion can all take place in a unified component called vector modulator (VM) downmixer. Moreover, by interchanging the mixer and the LNA, high level of self-interference to noise and distortion is attainable [56].

An ideal vector modulator is a device utilized to do the phase inversion on the input signal in addition to regulating the amplitude through controlling the in-phase and quadrature signal components. Figure 25 [57] shows that input signal is divided into two signals with quadrature phase apart from each other which are then affected by a control signal before being added in the adder block [58]. Figure 24 [52] represents a simple model of RF front-end architecture with a vector modulator downmixer [52].

In case of having two antennas, there are several methods of RF interference suppression which are examined in [22], [59]. Two different approaches are studied in [22]. In the first approach, a noise canceler chip is considered to remove the unwanted signal and have a clear signal at the receiver. This chip which is Quellen $QHx220$, is like a linkage between the transmitter antenna and the receiver antenna which performs the self-interference suppression while in the second approach, a nulling antenna is placed at the transmitter side to provide an extra amount of suppression. But the second approach is a passive cancellation technique [22].

$QHx220$ operates in the frequency scope of 300 MHz to 3 GHz with providing over 20 dB noise cancellation. This chip is utilized in many wireless devices due to the multiple advantages such as developing bit error rate (BER), receiver sensitivity through decreasing the amount of electromagnetic interference (EMI) signal, level of noise cancellation between adjacent channels and system performance. It is also able to remove both in-band and out-of-band interferers [60]. The internal block diagram of this chip is shown in Figure 26 [61]. A sampled noise corresponds to the noise of the target signal enters the input of this chip. In order to eliminate the electromagnetic interference signal and attain the signal integrity, an anti-noise signal is added to the target signal path [60]. VGAs signals are under the supervise of two digital-to-analog converters. Digital-to-analog converters are responsible for tuning the amplitude and phase of the cancellation signals. On the other hand, it has a non-linear characteristic in case of having over -45 dBm input signal which is significant concern in full duplex transceivers [60], [61].

There is also another way to provide the isolation between the TX and RX while using two separate antennas. In [59] two separate antennas which are located about 15-20 cm away from each other are employed in addition to a balanced or unbalanced balun transformer. This technique is suitable for high power systems which does not have bandwidth limitations. Balun which is a passive component is employed to invert an unbalanced signal to the balance signal and vice versa [61]. Baluns are used in modern communications such as RF, audio and video devices [59]. Signals at the output of a balun have equal powers but with 180° phase difference [61].

Authors in [59] have compared the level of SIC through employing a balun and phase offset techniques. They have considered two routes for transmission as the SI path and the cancellation path shown in Figure 27 [59]. The self-interference path includes a 20 dB attenuator and the second path has a tunable attenuator and a variable delay line in order to adjust the signal in the cancellation path in a way to match the SI signal. Finally, signals coming from both paths are added to the receiver. Transmitted signal is divided between these two paths through a balun and an RF splitter for signal inversion and phase offset cancellation methods respectively. They have shown that phase offset technique provides 50 dB and 25 dB cancellation for 5 MHz and 100 MHz signals respectively while in case of employing a balun, 52 dB suppression for 5 MHz signal and 40 dB suppression for 100 MHz signal is possible.

In addition to the benefits of balun, it is not frequency flat and so the signal is inverted with different magnitudes over the bandwidth. In this case, considering a constant attenuation and delay for the cancellation path does not suppress the SI signal properly [59].
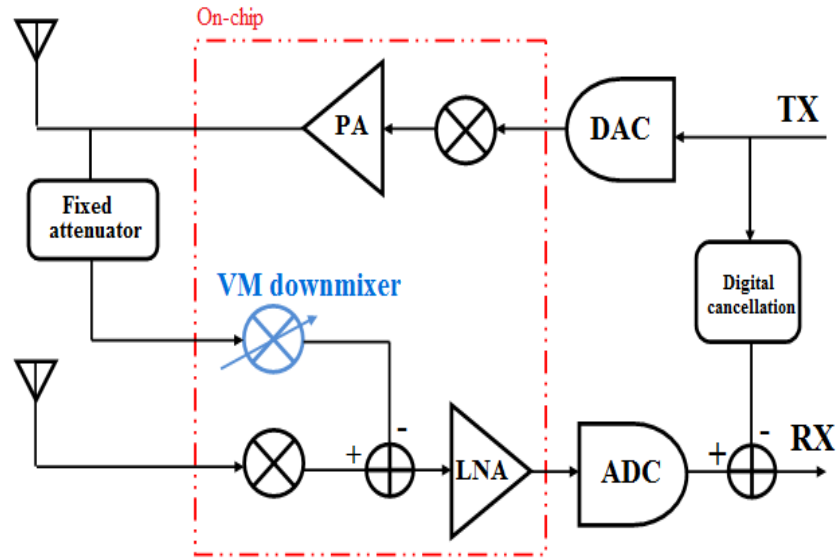
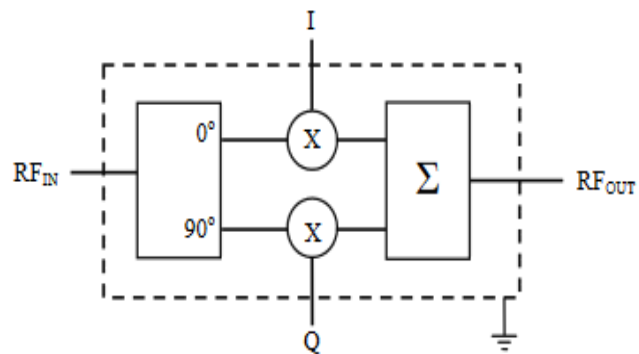Figure 24. Front-end model with a VM downmixer and a mixer before LNA.
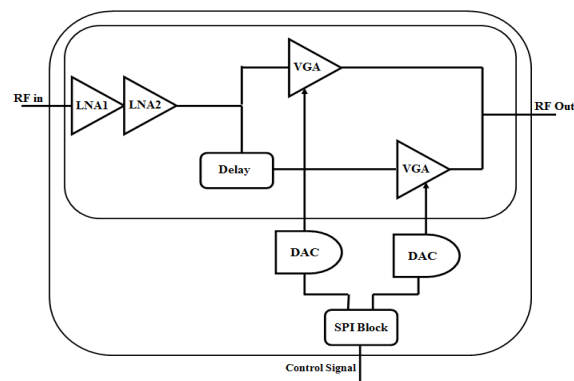

Figure 25. Configuration of the vector modulator.

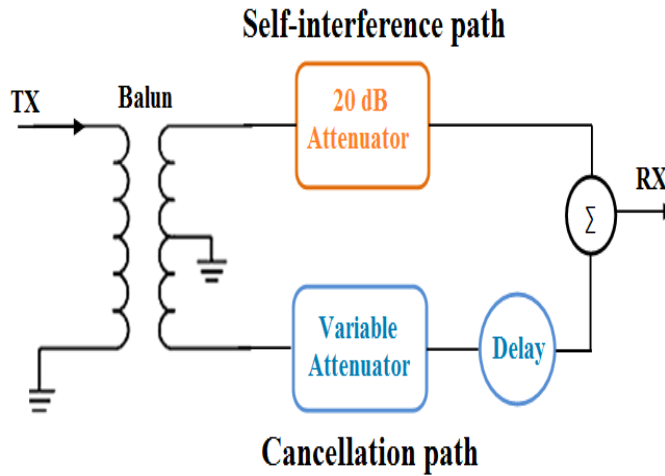Figure 26. $QHx220$ interior structure.

Figure 27. Block diagram of the system model with a balun transformer proposed and analog cancellation.

4.1.2. Dual Polarized Antenna

In full duplex technology, orthogonal polarization facilitates the transmission and reception at the same frequency and time. In case of applying a dual polarized antenna, both active and passive suppression techniques yield to a high isolation. Authors in [10] have applied two separate antennas in such way to have the orthogonal polarization. In several articles such as [23], [62], [63] and [64] designers have considered at least two antennas in their system models while in [18] a dual port antenna is considered as an alternative to the separate antennas. Since a dual polarized antenna has two ports with solitary elements of radiation, it is able to perform in horizontal and vertical polarizations simultaneously which means that the transmission takes place on one polarization and the reception is done through the other polarization simultaneously [52], [18]. One of the most interesting dual feed antennas is microstrip antenna which is cost efficient and easy to implement [18]. The most challenging issue in the dual feed antennas is overcoming the coupling between antenna ports since they are near to each other and cross coupling is also inevitable in this case [18]. Figure 28 [55] displays geometry of a dual polarized antenna from the top in addition to the multilayer case.

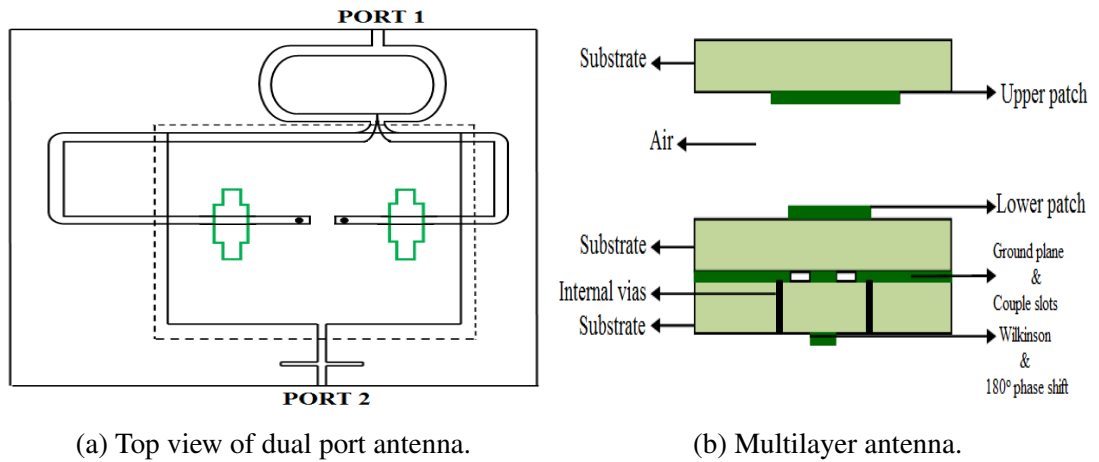(a) Top view of dual port antenna.　　　(b) Multilayer antenna.

Figure 28. Dual port antenna configuration.

Exterior factors lead to the variation of antenna's isolation. The level of SIC is reduced as a result of having the similar polarization in the received and reflected signals since the leakage signal is at the lowest level with an orthogonal polarization while the same polarization increases the power transmission from the transmitter to the receiver.

In case of having a single antenna shared between transmitter and receiver, authors in [26] have considered a particular antenna with having two feeds performing feed-forward suppression method. In this approach two circulators, two quadrature hybrids are utilized in addition to that single antenna with two feeds which cause to be a costly cancellation approach. There is also another way to utilize a single antenna which could be a general antenna.

In RF active analog cancellation with a dual polarized antenna as Figure 29 [52] illustrates, a copy of RF signal which is attenuated and phase inverted is added to the input of LNA. In case of having a desirable analog suppression, the RF signal and the cancellation signal are matched at the receiver and they have π phase difference [65]. This technique is also applicable with two separate antennas.
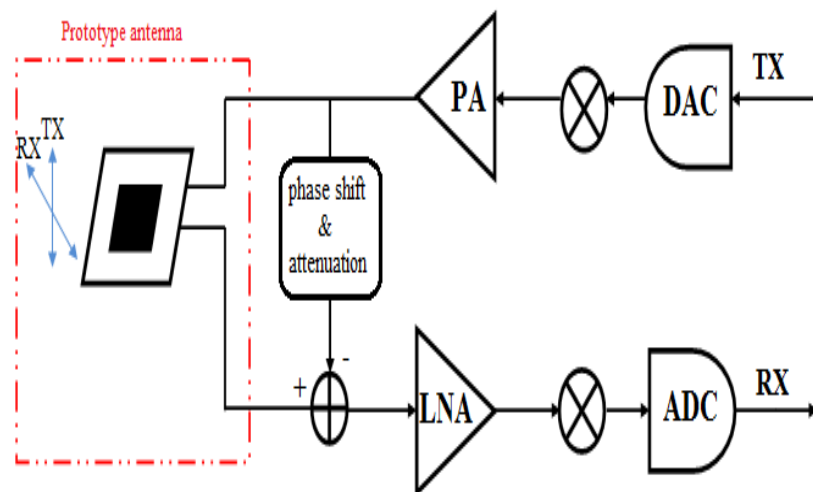

Figure 29. Dual-port antenna with active RF cancellation.

4.2. Active Cancellation Parameters

Authors in [65] have presented a way to find out values of phase shifting ϕ_c and attenuation α_c for active SIC in case of employing a common antenna with a circulator. If we assume s as the transmitted signal, s_c and s_t represent signals which pass through the cancellation path and antenna respectively. According to the Figure 30 [65] we have

$$s = Ax(t)e^{-j(wt+\phi_1)}. \tag{28}$$

Here, $x(t)$ is a unit signal with magnitude and angle of A and ϕ_1 respectively which is then suppressed by coupler's attenuation factor α_1.

$$s_t = (1 - \alpha_1)Ax(t)e^{-j(wt+\phi_1+\phi_2)}, \tag{29}$$

$$s_c = \alpha_1 Ax(t)e^{-j(wt+\phi_1+\phi_3)}. \tag{30}$$

Then part of the transferred signal attenuated by factor of $(1-\alpha_1)$, leaks to the receiver and affects by circulator's attenuation factor α_2.

$$s_{SI} = \alpha_2(1 - \alpha_1)Ax(t)e^{-j(wt+\phi_1+\phi_2+\phi_4)}. \tag{31}$$

Eventually, the received signal is determined as a combination of the intended signal (Y), self-interference signal and the cancellation signal.

$$r = Y + s_{SI} + \alpha_c s_c e^{-j(wt+\phi_c)}. \tag{32}$$

If $r = Y$, we can get a clear signal at the receiver chain. Therefore, we have

$$\alpha_2(1 - \alpha_1)Ax(t)e^{-j(wt+\phi_1+\phi_2+\phi_4)} = -\alpha_c\alpha_1 Ax(t)e^{-j(wt+\phi_1+\phi_3+\phi_c)}. \tag{33}$$

Cancellation chain can be designed based on the following α_c and ϕ_c.

$$\alpha_c = (1 - \alpha_1)\alpha_2/\alpha_1 \quad , \quad \phi_c = \phi_2 + \phi_4 - \phi_3 + \pi. \tag{34}$$

Since the environment condition is not stable during telecommunications, we should readjust the cancellation chain with any variation that occurs in the near field reflections. This is more essential for full duplex systems that work in an indoor environment since transmitter is affected by numerous close reflectors. This mechanism has to happen between each data transfer slot [17].
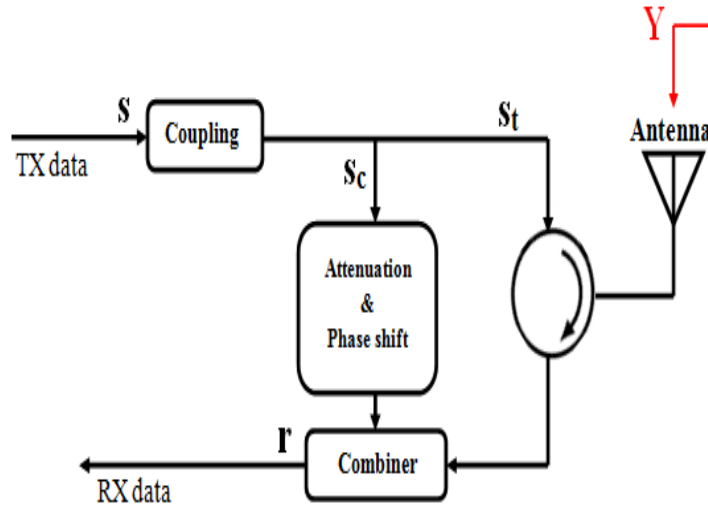
Figure 30. RF cancellation block diagram proposed for calculating the attenuation and phase shift for the cancellation path.

4.3. Antenna Polarization

Polarization which is also called wave polarization, is one of the main features in the wireless devices. Polarization is defined as the direction and magnitude of the electric field lines in an electromagnetic (EM) field. In case of having a specific direction of dispersion for all moments, polarization value would be constant while without determining the orientation, polarization varies per each wave period based on the maximum gain orientation [66]. In antenna theory, polarization is considered as the polarization of the radiated fields from the antenna [67]. Typically, when antennas have different polarization, there is an angle between the polarization vectors of the arriving wave and the receiving antenna which is known as polarization mismatch (polarization efficiency or loss factor). The amount of the receiving power is limited by this factor. Polarization mismatch leads to the loss in the received power and is expressed by polarization loss factor (PLF) [67], [61].

$$PLF = |\hat{\rho}_w . \hat{\rho}_a|^2 = |\cos \Psi_p|^2, \tag{35}$$

$$PLF(dB) = 20 \lg_{10} |\cos \Psi_p|, \tag{36}$$

where $\hat{\rho}_w$ and $\hat{\rho}_a$ are the polarization unit vectors of the incoming wave and the antenna respectively with the angle of Ψ_p between them which are shown in Figure 31 [67].
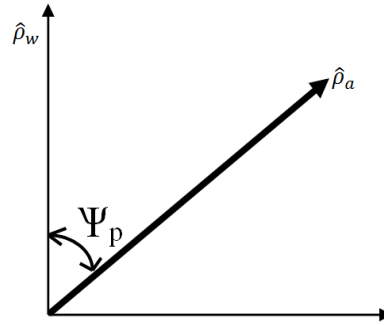
Figure 31. Comparative alignment of the polarization unit vectors of incoming wave and antenna.

As it was mentioned earlier in the introduction, if the TX and RX antennas have the orthogonal polarization according to each others requirement, no power from the transmitter enters the receiver which means that the isolation is ∞ or PLF is equal to zero or $-\infty$ [67]. The amount of isolation is limited by the polarization mismatch which is equal to PLF (dB) [61].

Recently orthogonal polarization specification of antennas have been considered in several full duplex literatures. Authors in [10] have examined orthogonal polarization through two separate antennas for transmitter and receiver which are located 35 cm away from each other while in [18] a dual port antenna is employed to generate the orthogonal polarization. Knowing the antenna's isolation besides the antenna polarization helps to figure out the amount of residual leakage signal which enters the receiver since its value depends on the amount of isolation provided between the antenna ports [18].

4.4. Recent Active SIC Techniques

Table 5 indicates total level of isolation achieved through recent RF self-interference cancellation methods applied in analog domain.

Table 5. Related RF analog SIC techniques

$Reference$	Isolation	Bandwidth
[65]	75 dB	10 MHz
[52]	62 dB	15 MHz
[55]	75 dB	10 MHz

4.5. Summary

In this chapter we studied active cancellation technique as the second SIC method in this thesis. This method is done in RF domain before ADC at the receiver chain. Active SIC is done through a secondary transmission chain which consists of a tunable attenuator and a tunable phase shifter. Isolation level according to the antenna polarization is also studied.

Level of the analog cancellation is restricted by some factors such as phase noise, nonlinear distortions, quantization error and IQ imbalance that we discussed earlier in Chapter 2 as transceiver impairments. Level of isolation attained by different related studies are also mentioned in this chapter.

5. NUMERICAL RESULTS

In Chapter 2, full duplex technology and its impairments have been discussed. Moreover, self-interference signal as one of the main concerns in full duplex systems and different methods to combat this interferer signal have been examined. In this chapter simulation results related to both self-interference cancellation techniques discussed in Chapter 3 and Chapter 4 are presented. First in Section 5.2 we start with working on electrical balance duplexer of IMEC design. The level of isolation is studied through tuning the tunable components exist in the balance network. Then in Section 5.3, results of the second method of cancellation, active analog cancellation is presented. It is also indicated how sensitive the isolation level is to the attenuation and phase shift variations.

5.1. Full Duplex Transceiver

In this thesis we worked on a FD transceiver which is shown in Figure 32, with three chains as transmitter, receiver and canceler. Transmitter chain is designed based on a direct conversion transmitter utilized in a typical full-duplex transceiver that upconverts the BB signal in the analog domain. The secondary chain is needed for the active cancellation and finally at the receiver chain, the intended received signal which has been affected by an unwanted self-interference faces a down conversion to be changed into the digital domain in the last stage of the receiving chain.

The digital baseband signal is created in MATLAB tool. MATLAB functions are embedded in the Advanced Design System (ADS) tool.

Thereupon, generated samples are entered into the ADS tool and pass through the transceiver branches and finally at the receiver chain, the analog signal is down converted to the baseband signal and then enters the MATLAB workspace where other signal processing takes place on the signal.

In Figure 32 we have considered a dual port antenna shared between the transmitter and the receiver which is suitable for 1.5 - 3.5 GHz bandwidth and provides more than 40 dB isolation. The main parameters considered in the transceiver design are listed in Table 6.

Table 6. RF system parameters for the model

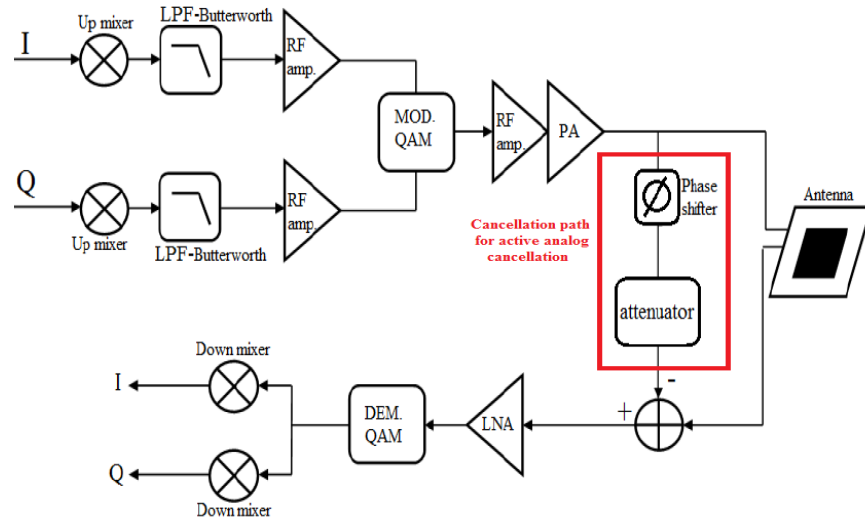| $Parameter$	Signal specification	Receiver	Transmitter (no PA)	Transmitter (with PA)	Unit
P_{out}			0	33	dBm
EVM			0.5	3.5	%
Noise level			-159	-158	dBm
Noise figure (NF)		2		2	dB
$IP3$		-4		50	dBm
ICP (-1dB)		-15		39	dBm
Bandwidth	20				MHz

Figure 32. Full duplex transceiver block diagram with active cancellation and a dual port antenna.

5.2. Electrical Balance Duplexer

As we mentioned earlier in Chapter 3, in a transceiver structure a single antenna shared between the transmitter and the receiver is desirable when we need a unified solution in case of having a limited antenna design space in full duplex systems. In this case, we could provide a good isolation between the transmitter and the receiver by employing an electrical balance duplexer. In this thesis, we have worked on the electrical balance duplexer according to the IMEC design shown in Figure 33. In EB architecture a 2.4 GHz dipole antenna shared between the TX and RX is utilized. Dipole antenna is widely used in radio communications due to the simple application and easy construction features.
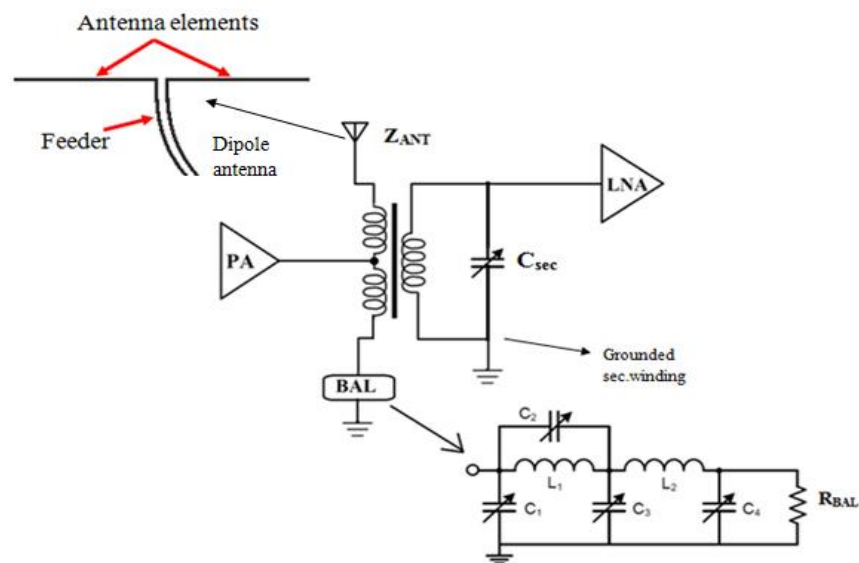

Figure 33. Electrical balance duplexer based on IMEC design.

As we discussed earlier, the main concern is to tune the balance network in a way to provide a good level of isolation. After designing the model in ADS, through the optimization process we found the optimal values required for a good TX-to-RX isolation. Then the sensitivity of the EB duplexer (EBD) to the variation of the tunable components in the balance network is examined.

The isolation is determined through the scattering parameters (s-parameters). S-parameters are ratios in dB which define the voltage ratios of the waves at incident, reflected or transmitted ports. In this thesis S_{21} indicates the amount of loss in the forward transmission path and the isolation is equal to the $|Loss|$ in dB.

Level of isolation attained after the balance network optimization is shown in Figure 34. All four tunable capacitors are tuned simultaneously. TX-to-RX isolation measured by S_{21} over 20 MHz bandwidth, shows that the electrical balance duplexer with a dipole antenna grants more than 60 dB isolation.

We optimize the balance network through the optimization simulation in ADS tool which works in a way to find out the determined performance goal. First we set up the optimization parameters such as optimizer type, simulation controller, a particular goal and the target component for the optimization process. The optimization runs until the optimization goal arrives then we update the model with the new optimized values for the enabled components. Here, we have considered 500 iterations.

Table 7 illustrates the optimization setup applied for the balance network and Table 8 shows obtained values of inductors and tunable capacitors after optimization of the balance network.

Table 7. Optimization setup for balance network

Optimization parameters	Display	Limit lines
Type	Gradient	
Goal	S_{21}	< -60 dB
Sweep variable	Frequency	1-3 GHz
Target component 1	Capacitors	0.1-1 pF
Target component 2	Inductors	1-2 nH

Table 8. Balance network components

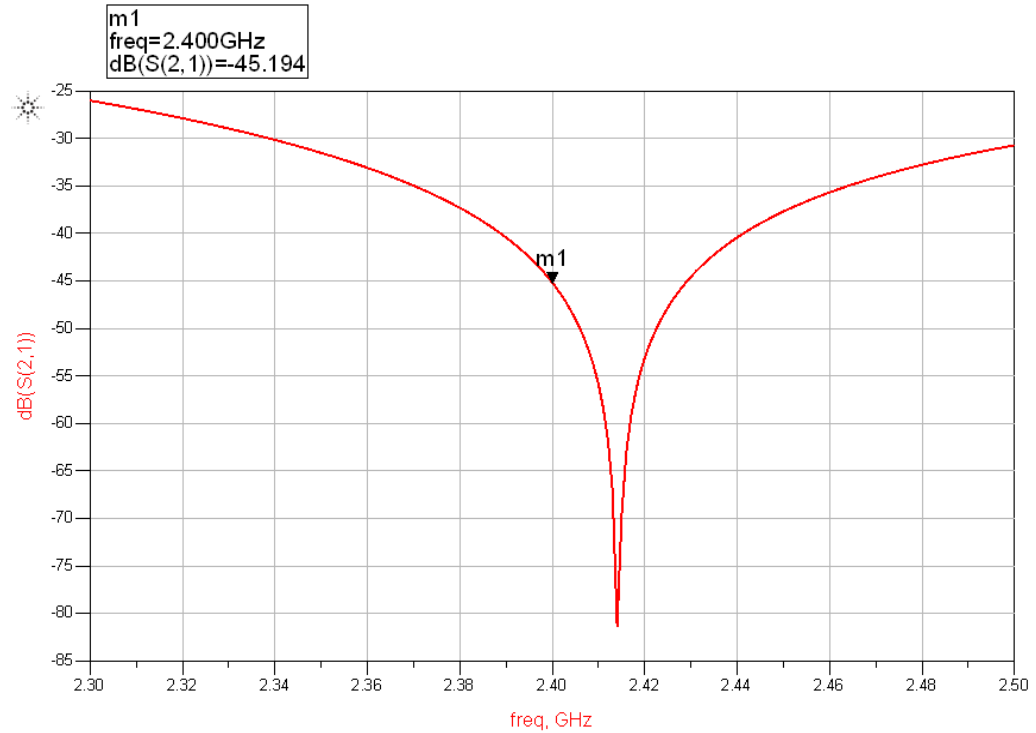| Component	Value	Unit
C_1	846.724	fF
C_2	1000	fF
C_3	1000	fF
C_4	200.032	fF
L_1	1.7	nH
L_2	1	nH

Figure 34. Level of isolation provided by electrical balance duplexer after the optimization of the balance network.

Figure 35 and Figure 36 indicate a dual notch TX-to-RX isolation in case of employing a dipole antenna which performs at 3 GHz. Notches are moved through sweeping the optimal values of the capacitors in order to figure out how to tune the isolation bandwidth and to identify which capacitor has the most impact on the frequency band of the isolation. In a sweep controller in ADS tool, we need to specify parameters such as sweeping type, sweeping parameters, start, stop and step points of the sweeping . In order to see the impact of the sweeping more clearly, we have considered few steps in the simulations. We have linearly increased and decreased the optimal values of each capacitor by 3 fF for 5 and 3 steps respectively.

Figure 35 and Figure 36 illustrate that decreasing or increasing values of the C_1, C_3 and C_4 tunes the level of isolation at each notch while the target frequency is controlled by the capacitor C_2 according to the balance network depicted in Figure 33. In all plots, the main curve related to the optimized values is labeled with markers m_1 and m_2 at each notch.
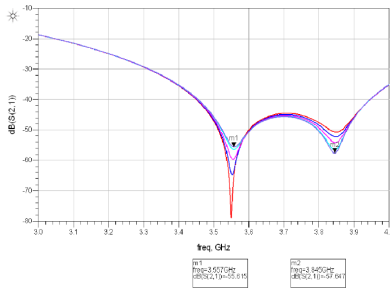
Resolution of the balancing resistor R_{BAL} and resonance bandwidth of the LC circuit of the balance network determine how deep notches can be in the frequency.
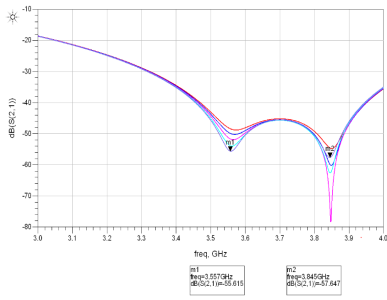
(a) Increasing value of C_1 by 3 fF for 5 steps.
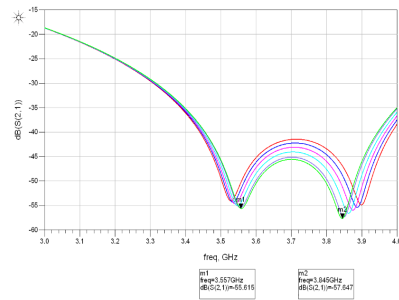
(b) Increasing value of C_2 by 3 fF for 5 steps.

(c) Increasing value of C_4 by 3 fF for 5 steps.

(d) Increasing value of C_3 by 3 fF for 5 steps.

Figure 35. Sensitivity of the isolation toward decreasing capacitors' optimal values by 3 fF.
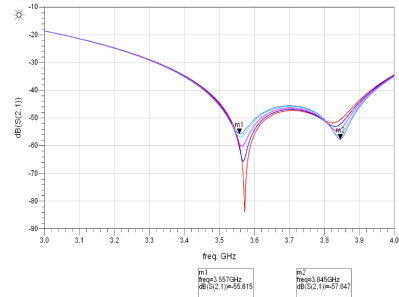

(a) Decreasing value of C_1 by 3 fF for 3 steps.

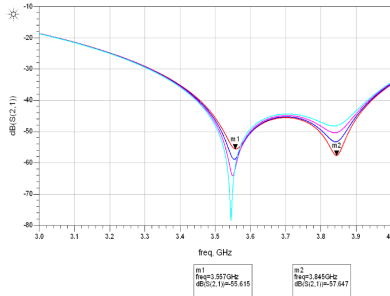(b) Decreasing value of C_2 by 3 fF for 3 steps.
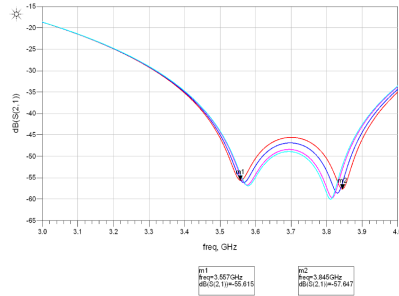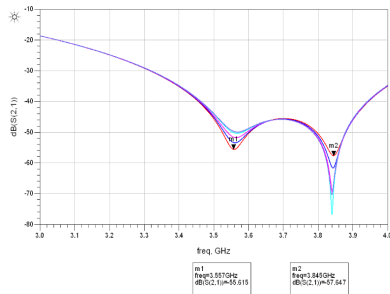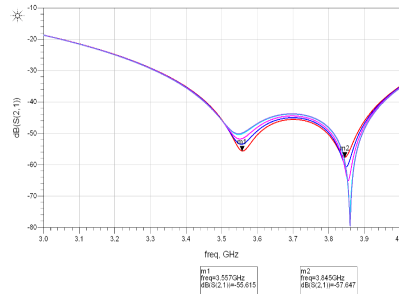
(c) Decreasing value of C_4 by 3 fF for 3 steps.

(d) Decreasing value of C_3 by 3 fF for 3 steps.

Figure 36. Sensitivity of the isolation toward increasing capacitors' optimal values by 3 fF.

Then we simulated the EBD model with an OFDM signal which is made in the Matlab workspace. The signal spectrum over 20 MHz bandwidth is measured after the power amplifier and before the low noise amplifier which means that the difference between these two signals determines the total level of isolation.
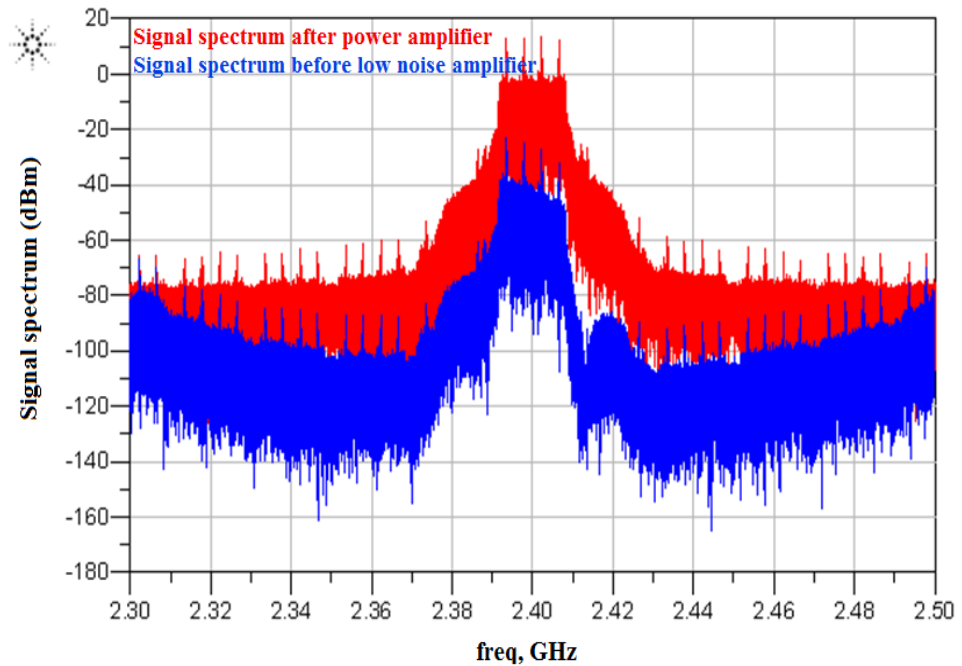
Figure 37. Signal spectrum before and after cancellation using EBD with an OFDM signal.

If we consider signal power after the PA and before the LNA according to the values measured as P_1 and P_2 equal to 32.661 (dBm) and -6.058 (dBm) respectively. The total isolation attained by the electrical balance duplexer is

$$\text{Total isolation (dB)} = |P_2 - P_1| = 38.719 \text{ dB}.$$

According to the Figure 34, electrical balance duplexer provides 45.194 dB isolation at 2.4 GHz while employing the EBD with the OFDM simulations represents lower level of isolation at the same frequency since the optimization has not provided the maximum level of isolation at 2.4 GHz so this total isolation value is much lower than the amount of isolation attained after the optimization.

5.3. Active Analog Cancellation

We take a replica of the signal after the power amplifier as the cancellation signal and it passes through a phase shifter and an attenuator before being added to the receiver chain. The considered cancellation path is indicated in Figure 32. Values of both attenuator and phase shifter are determined manually and via the optimization process. The isolation level attained for both cases (with manual and optimized values) is presented in this thesis.
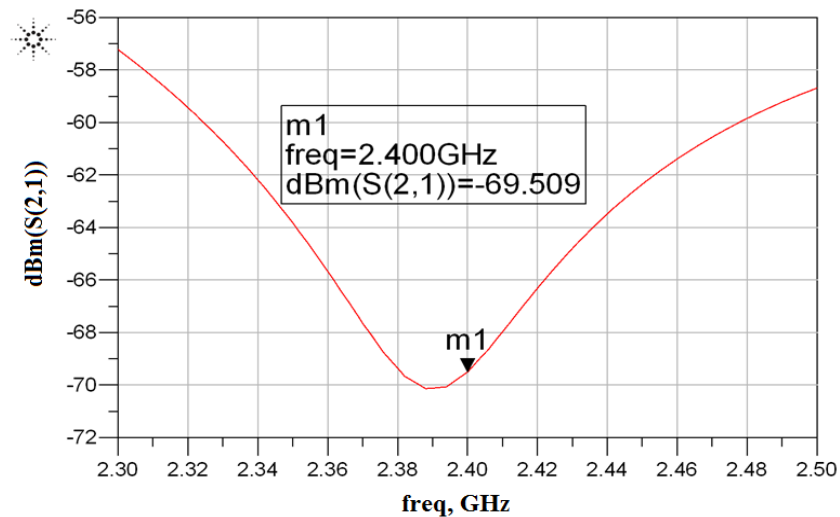
Figure 38. The isolation level obtained through the utilized dual port antenna.

In order to cancel the unwanted signal, the leaked signal and the cancellation signal should have 180° phase difference. We first need to find out the phase of the antenna at 2.4 GHz in order to determine the required phase shift for the cancellation signal. The attenuation value is assigned in such a way to have a good TX-to-RX isolation based on that specified phase shift. Since antenna's phase at 2.4 GHz is equal to -38.794^o, we set the phase shifter equal to 141.206^o and 78 dB attenuation obtained for the best case of TX-to-RX isolation level.
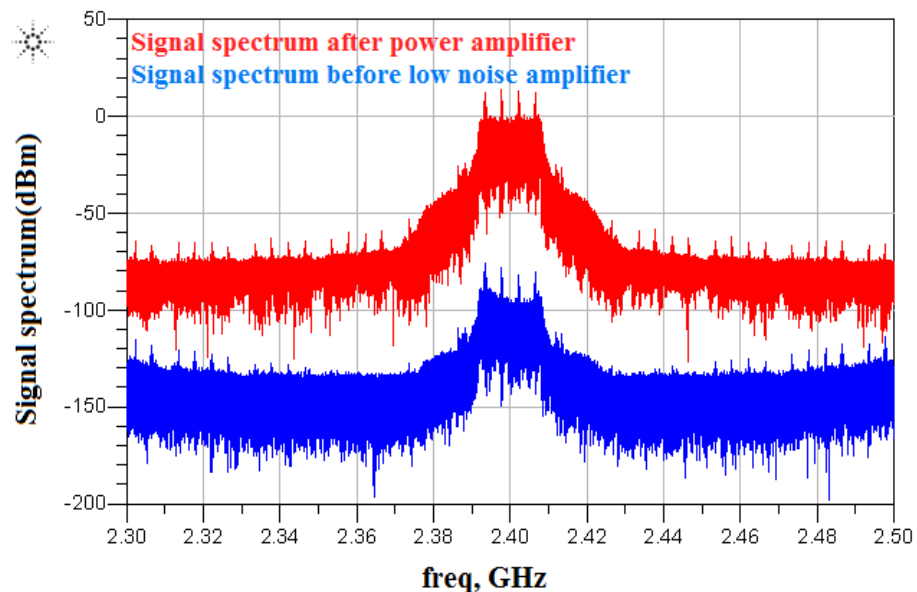
Figure 39. Signal spectrum before and after active cancellation over 20 MHz bandwidth with manual values of cancellation path. Attenuation is equal to 78 dB and phase shift is equal to 141.206^o.

In this case, 91.030 dB total isolation which is equal to the power difference between two curves in Figure 39 is achieved. According to the antenna isolation and comparing to the total achieved value, active cancellation has improved the isolation about 22 dB.

As we mentioned earlier, attenuation and phase shift values are also specified through the optimization process in the ADS tool since there are various combinations of the attenuation and phase shift for active cancellation. We were looking for the best combination which causes the maximum TX-to-RX isolation. Both phase and loss values were optimized simultaneously. Specifications of the optimization process are presented in Table 9. After several iterations and achieving the determined goal performance, we got very close optimal values to the manual ones which are 78.7435 dB and 145.846^o for attenuation and phase shift respectively. The simulation result and the level of cancellation after active cancellation is shown in Figure 40.

Table 9. Specifications of the optimization procedure of the attenuator and phase shifter

| *Optimization parameters*	Display	Limit lines
Type	Gradient	
Goal	S_{21}	<-70 dB
Sweep variable	Frequency	2-3 GHz
Target component 1	Attenuator	30-100 dB
Target component 2	Phase shifter	0°-360°
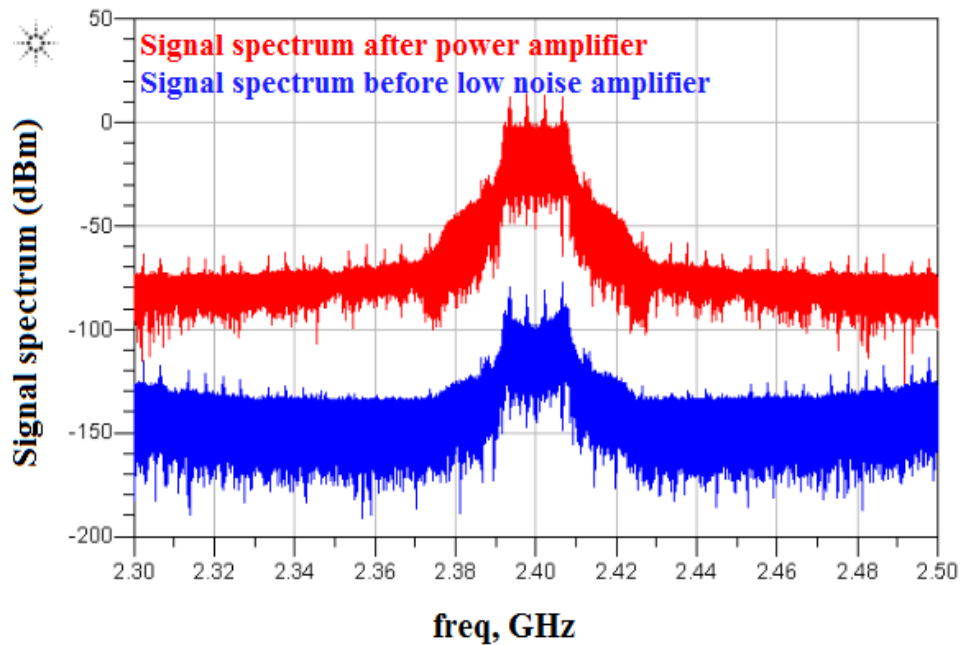
Figure 40. Signal spectrum before and after active cancellation over 20 MHz bandwidth with optimized values. Attenuation is equal to 78.7435 dB and phase shift is equal to 145.846^o.

Total isolation achieved with optimized values are approximately equal to the one obtained with manual values. Here, active analog suppression has improved the total isolation about 23 dB and 92.459 dB total isolation is attained.

In Figure 41 results of these two cases are compared through the s-parameter simulations.

(a) Optimized values. (b) Manual values.

Figure 41. Active analog cancellation with s-parameter simulation.

In order to see how far we could go from the optimized values of the RF cancellation, we have swept the optimized values of the attenuation 78.7435 dB and phase shift 145.846^o in the cancellation path of Figure 32 to see the isolation level alterations. Figure 42 represents different combinations of attenuation and phase shift.

attenuation	isolation
60.000	60.433
61.000	61.560
62.000	62.705
63.000	63.872
64.000	65.061
65.000	66.279
66.000	67.529
67.000	68.820
68.000	70.155
69.000	71.549
70.000	73.008
71.000	74.554
72.000	76.198
73.000	77.984
74.000	79.940
75.000	82.117
76.000	84.600
77.000	87.451
78.000	90.548
79.000	92.835
80.000	92.604
81.000	90.613
82.000	88.606
83.000	86.974
84.000	85.672
85.000	84.618
86.000	83.753
87.000	83.059
88.000	82.470
89.000	81.968
90.000	81.549

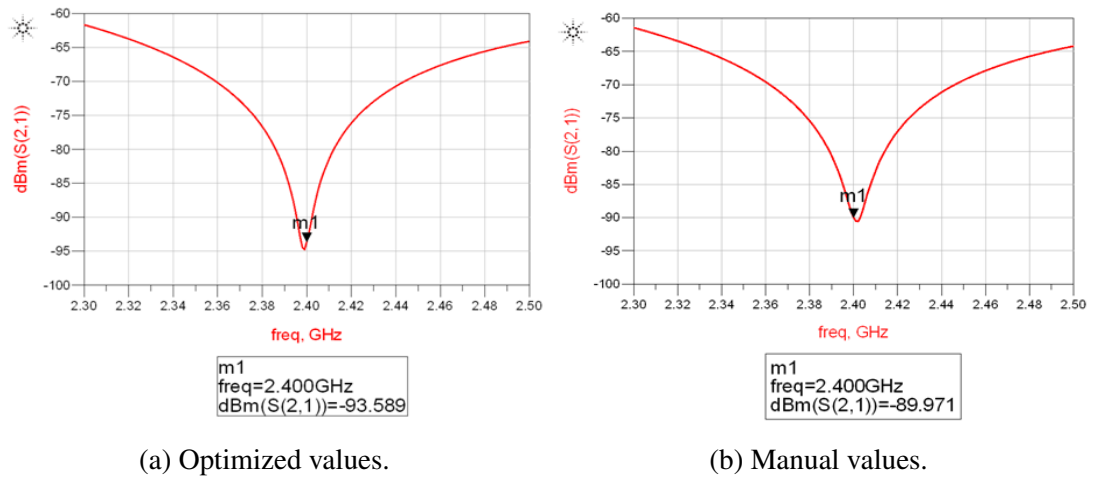| Phase shift	isolation
120.000	86.199
121.000	86.488
122.000	86.853
123.000	87.203
124.000	87.521
125.000	87.942
126.000	88.322
127.000	88.678
128.000	89.057
129.000	89.466
130.000	89.869
131.000	90.249
132.000	90.700
133.000	91.108
134.000	91.527
135.000	91.818
136.000	92.226
137.000	92.513
138.000	92.787
139.000	92.996
140.000	93.106
141.000	93.172
142.000	93.158
143.000	93.061
144.000	92.928
145.000	92.682
146.000	92.421
147.000	92.071
148.000	91.730
149.000	91.340
150.000	90.943
151.000	90.537
152.000	90.129
153.000	89.724
154.000	89.315
155.000	88.909
156.000	88.503
157.000	88.141
158.000	87.768
159.000	87.385
160.000	87.049

Figure 42. Isolation sensitivity towards variations of optimized values of attenuation and phase shift. Optimized values of attenuation and phase shift are equal to 78.7435 dB and 145.846^o respectively.

5.4. Summary

This thesis work discusses two RF SIC techniques, electrical balance duplexer and active analog suppression that each one has its own advantages and is suitable for different applications. These techniques are developed due to the need for having the integrity in compact radio systems. Here, the main specifications of these two methods are highlighted.

An electrical balance duplexer utilizes an adjustable electrical balance network and a single-port antenna for a simultaneous transmission and reception. This approach is frequency flexible since the level of SIC is tunable and we can find a good trade-off between the isolation and the operation bandwidth. It is also usable for digital and analog co-integration. According to the presented results for electrical balance duplexer, after optimization it provides about 45 dB isolation through the s-parameter simulations which is not the maximum level of isolation at 2.4 GHz carrier frequency.

On the other hand, with this technique > 3 dB loss occurs when the transmit power is divided between the antenna and the balance network through a hybrid transformer. Secondly, providing a wide bandwidth needed to enable the balance network to follow the variations of the antenna impedance is difficult to implement and also a tuning algorithm needs to be considered to support the impedance matching between the antenna and the balance network so the balance network resolution should be considered carefully in this method as well.

Active analog cancellation which works with a tunable cancellation chain and a dual port antenna provides almost 94 dB isolation in s-parameter simulations. Employed dual port antenna covers 1.5-3.5 GHz frequency range with impedance matching $<$-10 dB and more than 40 dB isolation. OFDM simulations represent around 93 dB total isolation where 23 dB out of that belongs to the active analog cancellation and the rest goes to the isolation provided by the utilized dual port antenna which is rather ideal and in practice this value is optimistic compared to actual measurements. Thus, high isolation is achievable over a large frequency scope.

Integration of compact radio devices is a significant concern in FD technology. Therefore, antenna structure becomes a serious issue in transceiver design and applying a proper SIC technique.

Although the simulation results indicate that the active analog cancellation with a dual feed antenna provides higher isolation in comparison with EBD, but in case of needing a denser integration, we need to employ a single-port antenna which exists in a very tiny size, instead of a dual port antenna with more complicated structure. Thus, each of which has its own merits in a two-way communication.

According to the specific parameters such as frequency flexibility, level of SI suppression, integration density and the isolation bandwidth discussed through the simulation results, we can design a suitable RF model for in-band full duplex systems.

6. CONCLUSIONS

In the recent years, full duplex technology has become an interesting topic since it works as a two-way communication which improves the link capacity and transmission security. Implementing full duplex communication is difficult due to the large unwanted signal at the receiver. For a desirable communication we need to suppress the unwanted signal to under the noise floor. In this chapter first we present a summary of the thesis. This is continued by a discussion about the work which we have done during this thesis. The aim of this thesis is to employ two RF cancellation techniques called electrical balance duplexer and active analog cancellation.

6.1. Summary

Chapter 2 presents an overview of the full duplex concept. Several factors leading to the generation of the self-interference signal such as duplexer leakage, impedance mismatch between the antenna and transmission line, and the environment reflections are studied. Then different architectures of the transmitter and receiver are compared together. This is followed by studying the impact of the transceiver impairments on the level of the jamming signal in the FD transceiver. In the following, different techniques in the analog and digital domains such as baseband cancellation, RF cancellation and antenna cancellation are examined in order to suppress the unwanted signal.

Chapter 3 discusses the electrical balance duplexer technique. EBD is applied for in-band full duplex systems as it provides an isolation between the transmitter and the receiver chains by canceling the self-interference signal. The cancellation is done with the help of the balance network which has four tunable capacitors. The balance network is tuned in such a way to follow the impedance variations of the antenna and provides the impedance matching between the antenna and the balance circuit. A 2.4 GHz dipole antenna is used in this architecture. The level of the isolation provided by the EBD depends on how well we can tune the balance network in order to keep the impedance matching between the antenna and the balance network. The isolation bandwidth is mainly tunable by one of the capacitors which is in parallel with an inductor.

Chapter 4 examines the active analog cancellation technique. In this method, a replica of the amplified signal at the RF domain passes through an attenuator and a phase shifter before being added to the the received signal at the receiver chain. In this technique, the unwanted signal is suppressed before the ADC in the RF domain. The level of the attenuation is determined by considering the fact that the cancellation signal has an identical magnitude as the received signal and phase shifter makes 180° phase difference between these two signals. The total isolation is provided by the antenna isolation and the active analog cancellation.

Chapter 5 provides some simulation results related to the two RF self-interference cancellation techniques studied in Chapter 3 and Chapter 4.

6.2. Discussion

Electrical balance duplexer works with a limited number of component non-idealities and a dipole antenna which provides more that 60 dB isolation across the channel bandwidth. In this technique according to the s-parameter simulations, about 45 dB isolation over 20 MHz bandwidth is attained while much lower isolation with the OFDM simulation is obtained since the balance circuit has not been optimized in such a way to provided the maximum isolation at the carrier frequency.

Active analog cancellation with optimized values of 78.743 dB attenuation and 145.846^o phase inversion in the cancellation chain, grants about 92 dB total isolation that 23 dB out of that belongs to the cancellation path and the rest goes to the isolation provided by the dual port antenna.

On the whole, the self-interference signal is not fully removed from the received signal and some amount of that exists as the residual self-interference signal. Therefore, the transmitted signal cannot go completely under the noise floor. In order to improve the isolation we need to employ cancellation techniques both in analog and digital domains. Self-interference signal highly depends on the TX power since with high transmit powers almost over 20 dB, the performance of all self-interference cancellation techniques commence to deteriorate. Nevertheless, the full duplex technology is still feasible to implement since it doubles the bandwidth efficiency and improves the transmission security.

7. REFERENCES

[1] Mikhael M., van Liempd B., Craninckx J., Guindi R. & Debaillie B. (2014) An in-band full-duplex transceiver prototype with an in-system automated tuning for rf self-interference cancellation. In: 1st International Conference on 5G for Ubiquitous Connectivity (5), 2014, IEEE, pp. 110–115.

[2] Abdelhalem S.H., Gudem P.S. & Larson L.E. (2014) Tunable cmos integrated duplexer with antenna impedance tracking and high isolation in the transmit and receive bands. IEEE Transactions on Microwave Theory and Techniques 62, pp. 2092–2104.

[3] (2014), When and where to use a duplexer. URL: http://blog.taitradio.com/2014/05/13/when-and-where-to-use-a-duplexer/.

[4] Diplexer vs duplexer-difference between diplexer and duplexer. URL: http://www.rfwireless-world.com/Terminology/diplexer-versus-duplexer.html.

[5] Van Liempd B., Craninckx J., Singh R., Reynaert P., Malotaux S. & Long J.R. (2014) A dual-notch+ 27dbm tx-power electrical-balance duplexer. In: European Solid State Circuits Conference (ESSCIRC), ESSCIRC 2014-40th, IEEE, pp. 463–466.

[6] Choi Y.S. & Shirani-Mehr H. (2013) Simultaneous transmission and reception: Algorithm, design and system level performance. IEEE Transactions on Wireless Communications 12, pp. 5992–6010.

[7] Xie X. & Zhang X. (2014) Does full-duplex double the capacity of wireless networks? In: INFOCOM, 2014 Proceedings IEEE, IEEE, pp. 253–261.

[8] Korpi D., Riihonen T., Syrjala V., Anttila L., Valkama M. & Wichman R. (2014) Full-duplex transceiver system calculations: Analysis of adc and linearity challenges. IEEE Transactions on Wireless Communications 13, pp. 3821–3836.

[9] Ahmed E. & Eltawil A. (2015) All-digital self-interference cancellation technique for full-duplex systems. IEEE Transactions on Wireless Communications 14, pp. 3519–3532.

[10] Everett E., Sahai A. & Sabharwal A. (2014) Passive self-interference suppression for full-duplex infrastructure nodes. IEEE Transactions on Wireless Communications 13, pp. 680–694.

[11] Kim D., Lee H. & Hong D.K. A survey of in-band full-duplex transmission: From the perspective of phy and mac layers .

[12] Sabharwal A., Schniter P., Guo D., Bliss D.W., Rangarajan S. & Wichman R. (2014) In-band full-duplex wireless: Challenges and opportunities. IEEE Journal on Selected Areas in Communications 32, pp. 1637–1652.

[13] Basheer B. & Mathews S. Active self interference cancellation techniques in full duplex communication systems-a survey .

[14] Choi J.I., Jain M., Srinivasan K., Levis P. & Katti S. (2010) Achieving single channel, full duplex wireless communication. In: Proceedings of the Sixteenth Annual International Conference on Mobile Computing and Networking, Mobi-Com '10, ACM, New York, NY, USA, pp. 1–12. URL: `http://doi.acm.org/10.1145/1859995.1859997`.

[15] Kolodziej K.E., Perry B.T. & Herd J.S. (2015) Simultaneous transmit and receive (star) system architecture using multiple analog cancellation layers , pp. 1–4.

[16] Duarte M., Sabharwal A., Aggarwal V., Jana R., Ramakrishnan K., Rice C.W. & Shankaranarayanan N. (2014) Design and characterization of a full-duplex multiantenna system for wifi networks. IEEE Transactions on Vehicular Technology 63, pp. 1160–1177.

[17] Bharadia D., McMilin E. & Katti S. (2013) Full duplex radios. In: ACM SIGCOMM Computer Communication Review, vol. 43, ACM, vol. 43, pp. 375–386.

[18] van Liempd B., Debaillie B., Craninckx J., Lavin C., Palacios C., Malotaux S., Long J.R., van den Broek D., Klumperink E. et al. (2014) Rf self-interference cancellation for full-duplex. In: 9th International Conference on Cognitive Radio Oriented Wireless Networks and Communications (CROWNCOM), 2014, IEEE, pp. 526–531.

[19] Best S.R. (1999) Antenna polarization considerations in wireless communications systems. Cushcraft Corporation 2002.

[20] Chen S., Beach M. & McGeehan J. (1998) Division-free duplex for wireless applications. Electronics Letters 34, pp. 147–148.

[21] Bliss D., Parker P. & Margetts A. (2007) Simultaneous transmission and reception for improved wireless network performance. In: IEEE/SP 14th Workshop on Statistical Signal Processing, 2007. SSP'07, IEEE, pp. 478–482.

[22] Radunovic B., Gunawardena D., Key P., Proutiere A., Singh N., Balan V. & Dejean G. (2010) Rethinking indoor wireless mesh design: Low power, low frequency, full-duplex. In: Fifth IEEE Workshop on Wireless Mesh Networks (WIMESH 2010),2010, IEEE, pp. 1–6.

[23] Choi J.I., Jain M., Srinivasan K., Levis P. & Katti S. (2010) Achieving single channel, full duplex wireless communication. In: Proceedings of the sixteenth annual international conference on Mobile computing and networking, ACM, pp. 1–12.

[24] Sahai A., Patel G. & Sabharwal A. (2012) Asynchronous full-duplex wireless. In: Fourth International Conference on Communication Systems and Networks (COMSNETS), 2012, IEEE, pp. 1–9.

[25] Sahai A., Patel G. & Sabharwal A. (2011) Pushing the limits of full-duplex: Design and real-time implementation. arXiv preprint arXiv:1107.0607 .

[26] Knox M.E. (2012) Single antenna full duplex communications using a common carrier. In: Wireless and Microwave Technology Conference (WAMICON), 2012 IEEE 13th Annual, IEEE, pp. 1–6.

[27] Huusari T. (2015) Analog RF cancellation of self interference in full-duplex transceivers. Master's thesis, Tampere University of Technology.

[28] Weeraddana P.C., Codreanu M., Latva-aho M. & Ephremides A. (2010) On the effect of self-interference cancelation in multihop wireless networks. EURASIP Journal on Wireless Communications and Networking 2010, pp. 1–10.

[29] Singh N., Gunawardena D., Proutiere A., Radunovic B., Balan H.V. & Key P. (2011) Efficient and fair mac for wireless networks with self-interference cancellation. In: International Symposium on Modeling and Optimization in Mobile, Ad Hoc and Wireless Networks (WiOpt), 2011, IEEE, pp. 94–101.

[30] Ellinger F. (2008) Radio frequency integrated circuits and technologies. Springer Science & Business Media.

[31] Razavi B. et al. (1999) Rf transmitter architectures and circuits. In: Proceedings of the IEEE Custom Integrated Circuits Conference, IEEE, pp. 197–204.

[32] Mirabbasi S. & Martin K. (2000) Classical and modern receiver architectures. Communications Magazine, IEEE 38, pp. 132–139.

[33] Anttila L., Korpi D., Syrjala V. & Valkama M. (2013) Cancellation of power amplifier induced nonlinear self-interference in full-duplex transceivers. In: 2013 Asilomar Conference on Signals, Systems and Computers, IEEE, pp. 1193–1198.

[34] Balatsoukas-Stimming A., Austin A.C., Belanovic P. & Burg A. (2015) Baseband and rf hardware impairments in full-duplex wireless systems: experimental characterisation and suppression. EURASIP Journal on Wireless Communications and Networking 2015, p. 1.

[35] Riihonen T., Mathecken P. & Wichman R. (2012) Effect of oscillator phase noise and processing delay in full-duplex ofdm repeaters. In: Conference Record of the Forty Sixth Asilomar Conference on Signals, Systems and Computers (ASILO-MAR), 2012, IEEE, pp. 1947–1951.

[36] Syrjala V., Valkama M., Anttila L., Riihonen T. & Korpi D. (2014) Analysis of oscillator phase-noise effects on self-interference cancellation in full-duplex ofdm radio transceivers. IEEE Transactions on Wireless Communications 13, pp. 2977–2990.

[37] Korpi D., Anttila L. & Valkama M. (2014) Feasibility of in-band full-duplex radio transceivers with imperfect rf components: analysis and enhanced cancellation algorithms. In: 9th International Conference on Cognitive Radio Oriented Wireless Networks and Communications (CROWNCOM), 2014, IEEE, pp. 532–538.

[38] Korpi D., Valkama M., Riihonen T. & Wichman R. (2013) Implementation challenges in full-duplex radio transceivers. In: Finnish URSI Convention on Radio Science.

[39] Gu Q. (2005) RF system design of transceivers for wireless communications. Springer Science & Business Media.

[40] Askar R., Kaiser T., Schubert B., Haustein T. & Keusgen W. (2014) Active self-interference cancellation mechanism for full-duplex wireless transceivers. In: 2014 9th International Conference on Cognitive Radio Oriented Wireless Networks and Communications (CROWNCOM), IEEE, pp. 539–544.

[41] Hua Y., Ma Y., Liang P. & Cirik A. (2013) Breaking the barrier of transmission noise in full-duplex radio. In: Military Communications Conference, MILCOM 2013-2013 IEEE, IEEE, pp. 1558–1563.

[42] Wu W.R. (2016), Full duplex communications. URL: `http://3gpptrend.cm.nctu.edu.tw/20160121/5.%E5%90%B3%E6%96%87%E6%A6%95%E6%95%99%E6%8E%88_2016-01-22%205G-and-IoT-N.pdf`.

[43] Balatsoukas-Stimming A., Belanovic P., Alexandris K. & Burg A. (2013) On self-interference suppression methods for low-complexity full-duplex mimo. In: Asilomar Conference on Signals, Systems and Computers, 2013, IEEE, pp. 992–997.

[44] Duarte M., Dick C. & Sabharwal A. (2012) Experiment-driven characterization of full-duplex wireless systems. IEEE Transactions on Wireless Communications 11, pp. 4296–4307.

[45] Aryafar E., Khojastepour M.A., Sundaresan K., Rangarajan S. & Chiang M. (2012) Midu: enabling mimo full duplex. In: Proceedings of the 18th annual international conference on Mobile computing and networking, ACM, pp. 257–268.

[46] Microwave rf circulators. URL: `http://www.everythingrf.com/browse/microwave-rf-circulators`.

[47] van Liempd B., Hershberg B., Raczkowski K., Ariumi S., Karthaus U., Bink K.F. & Craninckx J. (2015) 2.2 a+ 70dbm iip3 single-ended electrical-balance duplexer in 0.18 um soi cmos. In: Solid-State Circuits Conference-(ISSCC), 2015 IEEE International, IEEE, pp. 1–3.

[48] van Liempd B., Hershberg B., Debaillie B., Wambacq P. & Craninckx J. (2015) An electrical-balance duplexer for in-band full-duplex with<-85dbm in-band distortion at+ 10dbm tx-power. In: European Solid-State Circuits Conference (ESSCIRC), ESSCIRC 2015-41st, IEEE, pp. 176–179.

[49] Malotaux E. (2013) Full-Duplex CMOS Duplexer: Passive self-interference cancellation. Ph.D. thesis, TU Delft, Delft University of Technology.

[50] Sartori E.F. (1968) Hybrid transformers. IEEE Transactions on Parts, Materials and Packaging 4, pp. 59–66.

[51] Mikhemar M., Darabi H., Abidi A. et al. (2013) A multiband rf antenna duplexer on cmos: Design and performance. Solid-State Circuits, IEEE Journal of 48, pp. 2067–2077.

[52] Debaillie B., van den Broek D., Lavin C., van Liempd B., Klumperink E., Palacios C., Craninckx J. & Nauta B. (2015) Rf self-interference reduction techniques for compact full duplex radios. In: Vehicular Technology Conference (VTC Spring), 2015 IEEE 81st, IEEE, pp. 1–6.

[53] Elkholy M., Mikhemar M., Darabi H. & Entesari K. (2014) A 1.6–2.2 ghz 23dbm low loss integrated cmos duplexer. In: IEEE Proceedings of the Custom Integrated Circuits Conference (CICC), 2014, IEEE, pp. 1–4.

[54] Mikhemar M., Darabi H. & Abidi A. (2009) A tunable integrated duplexer with 50db isolation in 40nm cmos. In: Solid-State Circuits Conference-Digest of Technical Papers, 2009. ISSCC 2009. IEEE International, IEEE, pp. 386–387.

[55] Debaillie B., van den Broek D.J., Lavin C., van Liempd B., Klumperink E., Palacios C., Craninckx J., Nauta B., Parssinen A. et al. (2014) Analog/rf solutions enabling compact full-duplex radios. Selected Areas in Communications, IEEE Journal on 32, pp. 1662–1673.

[56] van den Broek D.J., Klumperink E.A. & Nauta B. (2015) An in-band full-duplex radio receiver with a passive vector modulator downmixer for self-interference cancellation. IEEE Journal of Solid-State Circuits 50, pp. 3003–3014.

[57] TOŠOVSKÝ P. & Valuch D. (2010) Improvement of rf vector modulator performance by feed-forward based calibration. RadioEngineering 19, p. 627.

[58] (2016), Vector modulator. URL: http://www.microwaves101.com/encyclopedias/vector-modulator.

[59] Jain M., Choi J.I., Kim T., Bharadia D., Seth S., Srinivasan K., Levis P., Katti S. & Sinha P. (2011) Practical, real-time, full duplex wireless. In: Proceedings of the 17th annual international conference on Mobile computing and networking, ACM, pp. 301–312.

[60] Qhx220: Active isolation enhancer and interference canceller. URL: http://www.intersil.com/content/dam/Intersil/documents/qhx2/qhx220.pdf.

[61] Sethi A. (2013) Self-interference channel and analog baseband cancellation for full duplex transceiver. Master's thesis, University of Oulu.

[62] Duarte M. (2012) Full-duplex wireless: Design, implementation and characterization. Ph.D. thesis, Rice University.

[63] Khandani A.K. (2013) Two-way (true full-duplex) wireless. In: 13th Canadian Workshop on Information Theory (CWIT), 2013, IEEE, pp. 33–38.

[64] Khojastepour M.A., Sundaresan K., Rangarajan S., Zhang X. & Barghi S. (2011) The case for antenna cancellation for scalable full-duplex wireless communications. In: Proceedings of the 10th ACM Workshop on Hot Topics in Networks, ACM, p. 17.

[65] Phungamngern N., Uthansakul P. & Uthansakul M. (2013) Digital and rf interference cancellation for single-channel full-duplex transceiver using a single antenna. In: 10th International Conference onElectrical Engineering/Electronics, Computer, Telecommunications and Information Technology (ECTI-CON), 2013, IEEE, pp. 1–5.

[66] Rouse M., Polarization (wave polarization). URL: `http://whatis.techtarget.com/definition/polarization-wave-polarization`.

[67] Balanis C.A. (2016) Antenna theory: analysis and design. John Wiley & Sons.